CHALMERS
UNIVERSITY OF TECHNOLOGY

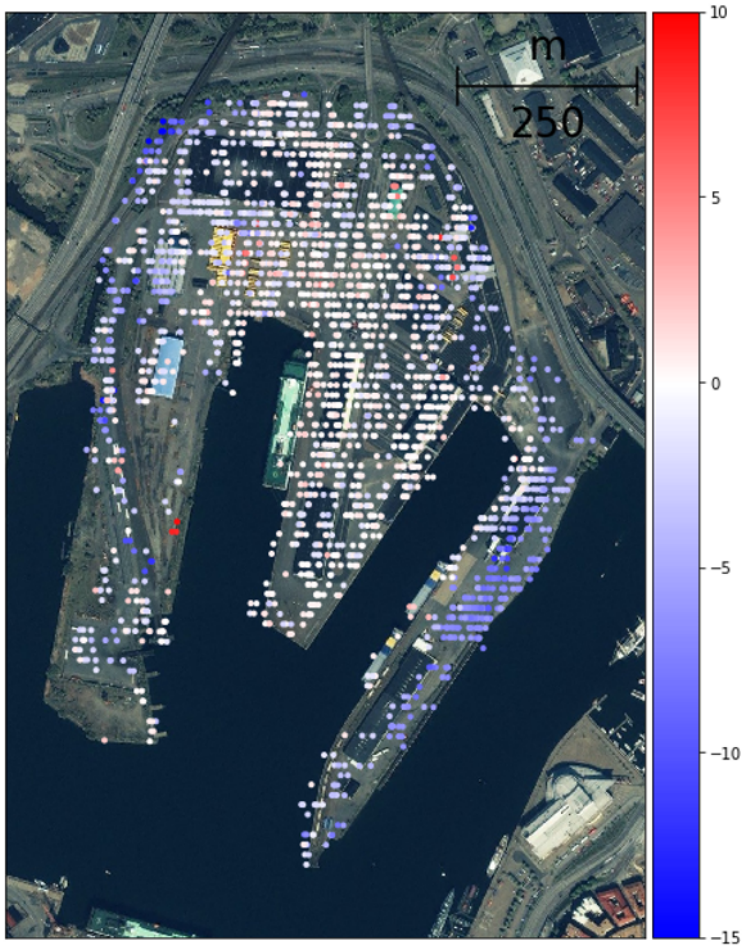

On the geotechnical capacities of Sentinel-1A InSAR measurements over the Gothenburg area

Master's thesis in Infrastructure and Environmental Engineering

MARCO QUINTI

Department of Architecture and Civil Engineering
CHALMERS UNIVERSITY OF TECHNOLOGY
Gothenburg, Sweden 2019

Master's thesis ACEX30-19-80

On the geotechnical capacities of Sentinel-1A InSAR measurements over the Gothenburg area

MARCO QUINTI

CHALMERS
UNIVERSITY OF TECHNOLOGY

Department of Architecture and Civil Engineering
Division of Geology and Geotechnics
Chalmers University of Technology
Gothenburg, Sweden 2019

On the geotechnical capacities of Sentinel-1A InSAR
measurements over the Gothenburg area
MARCO QUINTI

Supervisor: Jelke Dijkstra, Department of Architecture and Civil Engineering
Co-supervisor: Carolina Sellin, Department of Architecture and Civil Engineering
Industry Supervisor: Tommy Pap, Norconsult AB (Gothenburg)
Examiner: Jelke Dijkstra, Department of Architecture and Civil Engineering

Master's Thesis ACEX30-19-80
Department of Architecture and Civil Engineering
Chalmers University of Technology
SE-412 96 Gothenburg
Telephone +46 31 772 1000

Cover: Sentinel 1-A InSAR measurements over Frihamnen area (Gothenburg, Sweden) plotted on a color scale representing the mean vertical velocity of the points in [mm/year], where negative values indicate settlement.

Typeset in LaTeX
Gothenburg, Sweden 2019

On the geotechnical capacities of Sentinel-1A InSAR measurements over the Gothenburg area

MARCO QUINTI
Department of Architecture and Civil Engineering
Chalmers University of Technology

Abstract

The urban area of Gothenburg, Sweden, has always been strongly characterized by deformation of the soil underneath, due to the predominance of a soft material like clay in it. The focus of the present study has been the assessment of the potentialities of Sentinel-1A InSAR satellite measurements for monitoring and prediction of settlement, through a detailed comparison with traditional measurements like optical levelling and bellow hose gauges. The study has been carried out on two specific sites near the central part of the city of Gothenburg, Frihamnen and Nordstan/Centralen, chosen for their position, data availability, type and magnitude of deformation, after a comparison with other possible study sites. The investigation of the deformation has been done with synergy of other geo-informatics in the area, such as SGU (Sveriges Geologiska Undersökning) soil maps, groundwater levels and a CPTU database (property of Norconsult, Gothenburg) and has been based on a detailed literature review about the geotechnical concept of soil deformation and the different existing methods to measure and/or predict it. To assess the specific capacities of InSAR measurements, their statistical variations have been addressed and the accuracy of their results has been compared to traditional techniques both before and after filtering higher quality data points. This analysis has been carried out mainly using QGIS tools and the data science capabilities of Python programming. The results of this study show that the accuracy and precision of InSAR measurements for soil deformation monitoring is strongly related to the quality of data. The correspondence with measures from traditional methods does not appear to be satisfying when using entire InSAR data-sets with no selection, but is found to drastically increase when the low-quality data points are identified and excluded. In conclusion, InSAR proofs to be a serviceable and convenient tool for soil deformation monitoring and prediction, if object of a previous statistical analysis able to calibrate its measurements depending on their quality and to size their density and hence their reliability on large scale areas.

Keywords: soil deformation, InSAR, Sentinel-1A, settlement, clay, Gothenburg, geotechnical applications.

Acknowledgements

This thesis has been a collaboration between Norconsult in Gothenburg and Chalmers Division of Geology and Geotechnics.

I would like to dedicate my biggest thanks to my supervisor, Jelke Dijkstra for his motivational and coordinating assistance, to my tutor, Tommy Pap for his technical explanations and support and to my co-supervisor, Carolina Sellin for her friendly and dedicated help. This entire work would not have been possible without their knowledge, their experience and their competences. Thanks as well to all the professionals I have not directly come in contact with, but that in their own way have contributed to this work.

I also want to warmly thank my parents, my grandparents and all my family for their closeness during some hard and dark moments, especially dark during winter. A huge thanks goes to my friends too, the genuine laughs and levity moments they can give me so easily despite the distance, helped a lot.

Finally, I want to thank Francesca for her love, patience and the mutual support and motivation that characterized this long period of living together.

Marco Quinti, Gothenburg, June 2019

Contents

List of Figures

List of Tables

1

Introduction

1.1 Background

The geology of the subsurface underneath the city of Gothenburg, in South-Western Sweden, is composed of different materials, remaining of several glacial and glaciofluvial deposits, but there is a predominant share of soil consisting of glacial clay (SGU, 2019). This particular soft soil is responsible for what represents one of the main issues of the urbanization of Gothenburg and other cities built on the same soil type: the soil surface ongoing displacement.
This process is caused by consolidation and creep and represents a risk both for already built buildings and future constructions. Consolidation takes place, among others, when a soft soil is mechanically loaded with vertical loads like buildings, which cause a vertical movement of the surface as consequence of the volumetric deformation of the soil (Knappett and Craig, 2012). Consolidation is a time dependent process, for which the final displacement is easier to calculate and forecast than its time rate. The particular composition of the sub-surface underneath Gothenburg, related to its particular recent history of fillings and dredging near the riverbank areas, makes it even a harder job. This is in fact where the strength of satellite measurements comes into play, since they allow for measurements with a constant temporal rate, based on the orbit of the satellite, that is not relying on the accessibility of the specific site, also offering a huge database of data extended on several years, publicly and freely available.
The present study is focused on the Sentinel-1A InSAR satellite measurements with the overall aim to get a new insight on its capacities and peculiarities for geotechnical monitoring, based on a comparison with traditional measurements within two specific study sites, Frihamnen and Nordstan/Centralen. Many other studies on the application of SAR interferometry for soil displacement monitoring are publicly available. The difference from those is that the present study aims not only to demonstrate to what degree InSAR is a good and reliable methodology for such purpose, but also to study its usefulness as tool for settlement prediction. Furthermore, to assess in details InSAR's statistical parameters in order to assess its reliability, as explained in details in the following section.

1.2 Objectives and aims

The main aim of the present work is to assess the geotechnical usefulness of Sentinel-1A InSAR satellite measurements for soil displacement monitoring. The Thesis is focused on the central Gothenburg area and follows the objectives here formulated:

- The selection of the one or two best benchmark sites, based on a study on five possible ones, followed by a detailed geotechnical and geological description of them. This will take into consideration relevant factors like location, availability of data, type and magnitude of displacement.
- A comparison between settlement measurement coming from Sentinel-1A and traditional methods, followed by an analysis about their results' similarities and dissimilarities.
- Simple calculations of settlement starting from InSAR measurements, followed by a discussion to understand the potential use of InSAR measurements for prediction of settlement time and magnitude factors.
- An analysis of InSAR measure uncertainties and statistical variation and how they relate to this technique's reliability and to traditional geotechnical information.

2

Literature review

The focus of this review will not only be on the geotechnical subjects related to the soil and the process of consolidation, but also on the working process of the different methods to measure ongoing settlement or to predict it.

2.1 Soil composition and behaviour

Before analysing the process of soil displacement and its causes, it is important to understand how the soil is structured and what role is played by groundwater, since features of the consolidation of a particular soil are strongly related to the deposit's composition.

2.1.1 Characteristics of soil

The composition of soil can be described as a combination of a solid skeleton, consisting of the soil particles, and the void spaces in between these particles (Knappet and Craig, 2012). Depending on the kind of soil, on its history and on its surrounding conditions, not only the amount of void spaces can vary, but also the percentage of them that is filled with water. This is the reason why the composition of soil is often referred to as a three-phased structure, with material grains, air (compressible) and water (incompressible).
As stated by Knappet and Craig (2012), the presence of water in the soil has a critical impact on its behaviour, affecting fundamental processes like consolidation and heave, and that is why its role will be further discussed in Section 2.1.2.
When the soil is in its natural state, undisturbed, there is an equilibrium situation between the soil grains and both air and water contained in the voids in between; this equilibrium is disturbed when the soil is object of an external action. Any external event that results as a reason for a change in the natural soil equilibrium, will cause a reaction in the soil and will trigger a modification of the relationships among the three phases (Atkinson, 2007). The present case considers urbanization as a cause of change in soil equilibrium, but these actions are not only related to human beings, since geological and meteorological processes can affect it as well. This is in fact why the loading history of a soil plays such an important role in its characterization.

When a change in the state of equilibrium of the soil takes place, related to a loading or unloading situation, there can be two different ways in which the soil reacts, known as drained and undrained behaviours (Knappet and Craig, 2012). In order to understand the difference between them, there is the need to introduce the

concept of stress in soil. According to the definition given by Terzaghi and Fröhlich (1936), the stress that characterizes the soil can be divided in effective stress, σ', which is the stress acting only on the grains of soil material, and pore pressure, u, that is the stress acting on the water particles. The total stress, σ, is defined as the sum of the previous two stresses and hence their relation can be indicated as in Equation 2.1.

$$\sigma' = \sigma - u \tag{2.1}$$

Now that is clear what stresses are present in the soil and how they act, it is possible to go back to the difference between drained and undrained behaviour and, to do that, the focus will from now on be on the loading case, that is the object of this study. When a soil is vertically loaded, the magnitude of the load will correspond to an equivalent change in total stress of the soil. Initially, the load is taken by the pore water, as an extra pore pressure, afterwards it is transferred from the water to the soil particles, resulting in an increment of effective stress (Das, 2007).
According to Knappet and Craig (2012), the drained behaviour, also referred to as long-term case, is the situation occurring when the load has been completely transferred to the soil particles. On the contrary, the undrained behaviour, also known as short-term case, takes place when the dissipation of the extra pore water pressure in not started yet. These concepts are at the base of the consolidation process and will hence be further discussed in Section 2.2.

One of the main differences between coarse-grained soils (i.e. gravel) and fine-grained soil (i.e. clay) stands exactly there, in which behaviour they follow. The first, characterized by a higher hydraulic conductivity, allow the extra pore water pressure to dissipate faster, hence behaving as drained. The fine-grained soils, also referred to as soft soils, show on the contrary a much slower process of dissipation of excess pore water pressure, leading to an undrained behaviour (Knappet and Craig, 2012). Gothenburg clay is no exception in this, being easily object of consolidation and creep, as further discussed in Section 2.2.

2.1.2 Pore pressure

As introduced above, the role of ground water is extremely important when it comes to what to expect from the soil behaviour, thus a critical step during a geotechnical analysis is to investigate its features. The presence of water in the soil is in general regulated by the depth of what is called the ground water head: below that level, the soil is saturated with water, while above it the soil is partially saturated and/or dry. In an undisturbed situation of equilibrium, the soil below the ground water head will have a positive pore pressure, defined static, u_s, whose magnitude depends on the depth from the head level. When a loading or unloading action changes the equilibrium, an excess pore pressure, u_e, will be summed to the static one (Kempfert and Gebreselassie, 2006), respectively increasing or decreasing it. Now it is clear how the pore pressure introduced in Subsection 2.1.1 is composed, as shown below in Equation 2.2.

$$u = u_s + u_e \tag{2.2}$$

When the soil is loaded, hence a positive excess pore pressure is developed, the system will tend to go back to the equilibrium dissipating the u_e. This process occurs through the drainage of pore water from high pressure points towards lower pressure ones. In conclusion, dissipation of u_e is thus strictly dependent on the permeability and drainage conditions of the soil (Kempfert and Gebreselassie, 2006) and on its stiffness.

2.2 Soil displacement

Soil settlement linked to the process of consolidation is a main concern for a city like Gothenburg, mainly built on clay. This section is devoted to a detailed explanation of what is consolidation, how it can be predicted and what is needed for such calculation.

2.2.1 Definition of consolidation

According to Knappet and Craig (2012), consolidation is the gradual reduction in volume of a fully saturated soil of low permeability due to change in effective stress. As introduced above, the increase in effective stress is a consequence of the drainage of some of the pore water, set up by an increase in total stress. Since the in situ stress increases with depth, the stress increment perception decreases with depth, leading the local settlement to do the same. The process continues until the excess pore pressure has completely dissipated (Knappet and Craig, 2012). While the load is transferred from pore water to soil grains, these will rearrange their structure under the action of the increasing load, leading to a reduction in volume. Consolidation settlement is in fact defined as the vertical displacement of the soil surface corresponding to this volume change (Knappet and Craig, 2012).

As stated by Dinesh (2011), total settlement, S_t, is the sum of three components:

- Immediate settlement, S_i
- Primary consolidation settlement, S_c
- Secondary consolidation settlement, S_{sc}

The immediate settlement is regulated by the elastic theory and takes place immediately after the load is applied. This process is not time dependent and is characterized by a change in shape of the soil particles at constant volume, since the flow of pore water is negligible in low permeable soils and quick in high permeable ones (Dinesh, 2011).

The primary consolidation settlement is the main settlement process, responsible for the largest displacement share. It is a time dependent process that, as already introduced, depends on the drainage of pore water due to the creation of a hydraulic

gradient. Initially, the increment in total stress related to loading of the soil corresponds to an equal increment of pore pressure. Water is however incompressible, so the displacement of the soil does not start until the drainage of pore water does. From this moment, the excess pore pressure is slowly decreased and the load transferred to soil grains through an increased effective stress (Figure 2.1). The increment of σ' generates the change in volume of the soil due to particles rearrangement (Dinesh, 2011) with a reduction of void ratio. The ratio of displacement is maximum at the beginning and decreases with time, continuing until the u_e (Δu in Figure 2.1) is totally dissipated.

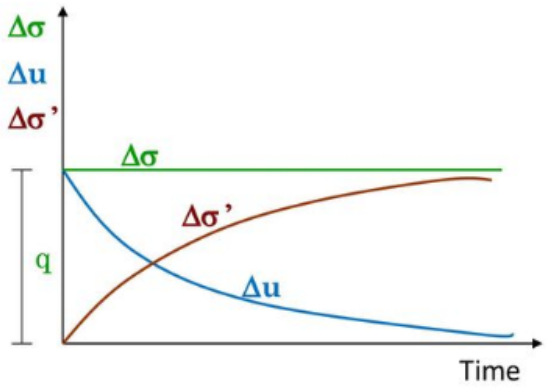

Figure 2.1: Total stress, effective stress and pore pressure behaviour during consolidation (q being the load)

The secondary consolidation settlement, also known as creep, is a compression process that continues under constant effective stress, when primary consolidation is completed. It is a time dependent process, with a ratio that decreases in time, but its displacement magnitude is smaller (there are some exceptions) compared to primary consolidation (Dinesh, 2011). According to Knappet and Craig (2012), secondary consolidation is thought to be due to the gradual readjustment of fine-grained particles into a more stable structure, following the void ratio decrement.

2.2.2 Specific needs to predict consolidation

Despite time passing and research going on, Terzaghi's theory of 1D consolidation remains one of the most widely used method for predicting consolidation. This theory will be used in the present subsection to introduce the reader to the parameters needed for consolidation prediction. It is important to state though, that most of the flow problems in the subsurface happen on a 3D level, going well beyond the 1D simplification. The fourth assumption presented below is in fact often denied in the real case. Despite this, Terzaghi's theory remains a useful tool to introduce the concept of consolidation.

Relating the three quantities excess pore water pressure, depth from top of soil layer (z) and time from the total stress increment (t), Terzaghi (1943) developed an analytical model to determine the degree of consolidation of soil at any time, that

is based on the following assumptions (Knappet and Craig, 2012):

- Homogeneous soil
- Fully saturated soil
- Incompressible solid particles and water
- 1D (vertical) compression and flow
- Small strains
- Darcy's law always valid
- Hydraulic conductivity and coefficient of volume compressibility remain constant during the process
- Unique relation, independent of time, between void ratio and effective stress

According to Knappet and Craig (2012), Terzaghi proposed the following differential equation (2.3) to solve its model:

$$m_v \frac{\mathrm{d}u_e}{\mathrm{d}t} = \frac{k}{\gamma_w} \frac{\mathrm{d}^2 u_e}{\mathrm{d}z^2} \tag{2.3}$$

where m_v is the coefficient of volume compressibility, k is the hydraulic conductivity and γ_w is the unit weight of water. Equation 2.3 can be rewritten as presented in Equation 2.4 below, that shows the above mentioned relation among excess pore pressure, depth and time:

$$\frac{\mathrm{d}u_e}{\mathrm{d}t} = c_v \frac{\mathrm{d}^2 u_e}{\mathrm{d}z^2} \tag{2.4}$$

where c_v is called coefficient of consolidation and is defined as in Equation 2.5, where β is the compressibility of water. Since both k and m_v are assumed to be constant and β to be null, c_v remains constant during consolidation.

$$c_v = \frac{k}{\gamma_w (m_v + n\beta)} \tag{2.5}$$

One of the main advantage of Terzaghi's theory is that, as introduced above, it permits to predict not only the total amount of settlement and the time needed to reach it, but also the degree of consolidation after a certain time. That can be really useful when it comes for example to the expected life time of foundations of a building, where correlating the soil displacement with the time factor can be critical. To explain that, the introduction of two new parameters is needed, presented in Equations 2.6 (Knappet and Craig, 2012) and 2.7 (Verruijt & Van Baars, 2007) below .

$$T_v = \frac{c_v t}{d^2} \tag{2.6}$$

T_v is a dimensionless number called time factor and d (also called H) is the maximum drainage path for pore water. If the consolidating layer is open (both upper and lower boundaries open for drainage), d equals half of its thickness; if the layer is half-closed (only one boundary is open), d equals the thickness of the layer.

$$U_{\mathrm{v}} = \begin{cases} 2\sqrt{\frac{T_v}{\pi}} & T_v < 0.2 \\ 1 - \frac{8}{\pi^2} \sum_{j=i}^{\infty} \frac{1}{(2j-1)^2} e^{-T_v \frac{\pi^2}{4}(2j-1)^2} & T_v > 0.2 \end{cases} \tag{2.7}$$

U_v is defined as average degree of consolidation and is of practical interest because, when multiplied by the total predicted settlement, it indicates the amount of settlement corresponding to the time t. Figure 2.2 below shows how the time factor and the average degree of consolidation are related. The three curves represent the different cases of initial conditions in the oedometer test (1), normal consolidation (2) and field condition when a surface loading is applied (3).

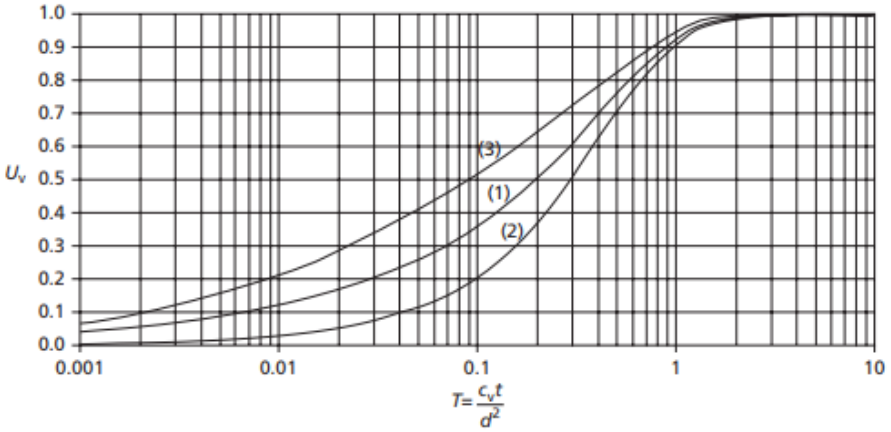

Figure 2.2: Relationships between T_v and U_v depending on the initial variations of excess pore water pressure (Knappet and Craig, 2012)

Now that the 1D consolidation theory has been introduced, it should be clear how, according to Equation 2.4 and 2.5, some of the most important parameters for the prediction of consolidation settlement are hydraulic conductivity, coefficient of consolidation and, consequently, coefficient of volume compressibility. The k regulates the velocity of pore water drainage and hence the one of the whole process, c_v describes the behaviour of consolidation with the unit [m^2/year] and m_v indicates the ratio of volumetric strain to applied stress [m^2/MN] (Knappet and Craig, 2012) and is furthermore needed to retrieve c_v. The pre-consolidation pressure, σ'_c, representing the maximum pressure that the soil has undergone during its history, is also a critical parameter for the determination of consolidation settlement. This value is in fact compared to the in situ effective stress, as shown in Equation 2.8 below, to calculate the so-called over-consolidation ratio, OCR.

$$OCR = \frac{\sigma'_c}{\sigma'} \tag{2.8}$$

This parameter results explanatory for one soil's consolidation since, considering the same type of grain size, a normally consolidated soil (OCR=1) tends to settle much more than an over-consolidated one (OCR>1). The reason for this is that an over-consolidated soil has already undergone an increased effective stress and hence has already settled (partly or totally). In conclusion, since primary consolidation settlement causes plastic deformations (Dinesh, 2011), these don't "disappear" after the unloading of what caused them.

Two valid laboratory tests to retrieve the above mentioned parameters are the

constant rate of strain (CRS), common in Sweden, and the incremental loading oedometer test. According to Moritz (1995), during a CRS test a constant rate of displacement is applied to an undisturbed soil sample, with constant cross-section area. The vertical load needed to consolidate the specimen is measured continuously. On the contrary, through an oedometer test the soil sample undergoes different loading steps of known load increment (always doubling the previous one) followed by dissipation of pore water pressures and the strain is measured (Knappet and Craig, 2012). In both tests the soil sample is laterally constrained and the displacement is vertical.

2.2.3 Asaoka's method

The one-dimensional consolidation theory is a valuable and useful tool to calculate soil's settlement behaviour in many cases in practical foundation engineering. Nevertheless, there are complications related to its use both due to its assumptions, which as seen are not always verified in the real case, and due to a certain degree of uncertainty when it comes to the calculation of needed parameters like coefficient of consolidation, excess pore water pressure and drainage path, for which an expert judgement is often requested (Asaoka, 1978). For these reasons, depending on the situation, sometimes what is called the "observational procedure" happens to be preferred in practical applications.

The "observational procedure" is a settlement predicting method introduced by A. Asaoka in 1978, that is based on the concept of forecasting soil's settlement at any time, including the infinite one, starting from the settlement observations available for that soil deposit. This procedure presents two variants, a graphical method and a method based on the Bayesian inference of a non stationary stochastic process (Asaoka, 1978). The last one allows to define a predictive probability distribution of future settlement, but it will not be further discussed since for the present study the graphical method is used, due to its simplicity.

In general, Equation 2.9 can be used to express the settlement of a clay layer for any boundary condition:

$$\rho(t) = \int_0^H \varepsilon(t, z)dz \tag{2.9}$$

where $\rho(t)$ indicates the settlement at time t, H is the thickness of the layer and $\varepsilon(z,t)$ is the vertical strain at time t and depth z. Substituting the raw solution of the original one-dimensional consolidation differential equation (2.3) in 2.9, with respect to t, a set of equations will be obtained, which can be approximated with the following n^{th} order in Equation 2.10, adopted as a master equation of settlement-time relationship (Asaoka, 1978):

$$\rho + c_1\dot{\rho} + c_2\ddot{\rho} + ... + c_{\mathrm{n}}\overset{(n)}{\rho} = C \tag{2.10}$$

where $c_1, c_2, \ldots, c_n$ and C (final settlement) are regarded as unknown constants and the upper points represent time-differentiation. Considering a discrete time $t_j = \Delta(t) * j$, with j=1,2,3... and a constant $\Delta(t)$, Equation 2.10 can be reduced to the difference form 2.11 that gives an idea of observational settlement prediction:

$$\rho_{\mathrm{j}} = \beta_0 + \sum_{s=1}^{n} \beta_{\mathrm{s}} \rho_{\mathrm{j-s}} \tag{2.11}$$

in which ρ_j indicates the settlement at time $t=t_j$ and coefficients β_0 and β_s are unknown parameters. The first order difference equation

$$\rho_{\mathrm{j}} = \beta_0 + \beta_1 \rho_{\mathrm{j-1}} \tag{2.12}$$

can be used to substitute the stable state $\rho_j = \rho_{j-1} = \rho_f$, representing the final settlement, to obtain the following:

$$\rho_{\mathrm{f}} = \frac{\beta_0}{1 - \beta_1} \tag{2.13}$$

Equations 2.12 and 2.13 allow to respectively predict the settlement at time $t=t_j$ (explained below) and $t=\infty$, where the values of β_0 and β_1 can be calculated through the following graphical method.

For the graphical procedure of what is also called Asaoka's method, the first step is to plot the settlement observations available against time, as shown in Figure 2.3.

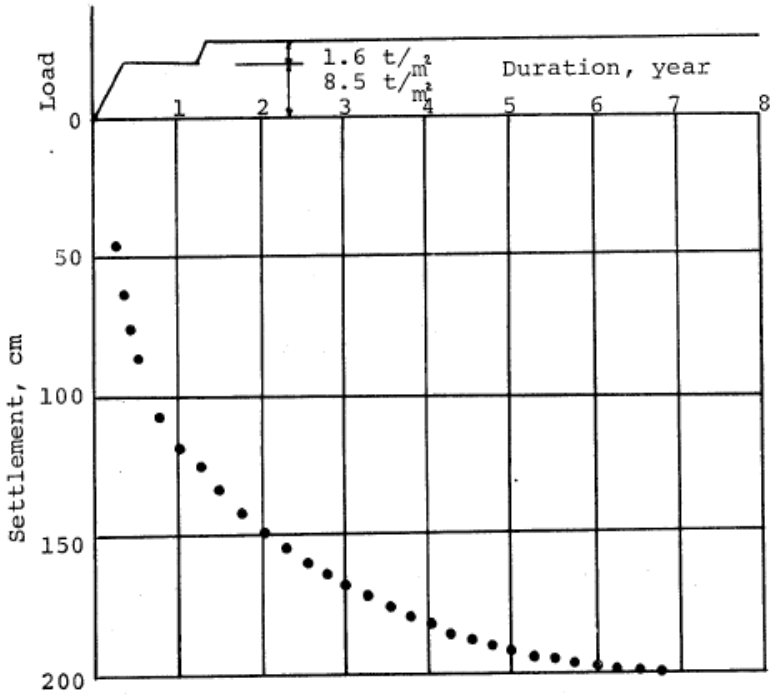

Figure 2.3: Settlement measurements from a real case study (Asaoka, 1978)

Now it is possible to define a constant time interval, $\Delta(t)$, and to extract the settlement values $\rho_1, \rho_2, \rho_3 \ldots$ corresponding to the times $t_1, t_2, t_3 \ldots$ which are defined

as ρ_j. Same procedure is used to extract the values of settlements starting from the previous time interval (ρ_0, ρ_1, ρ_2...), that will hence be defined as ρ_{j-1}. Plotting ρ_j and ρ_{j-1} on a graph as y-axis and x-axis respectively, the result will be similar to Figure 2.4, where a $x = y$ line (outlined) has been added.

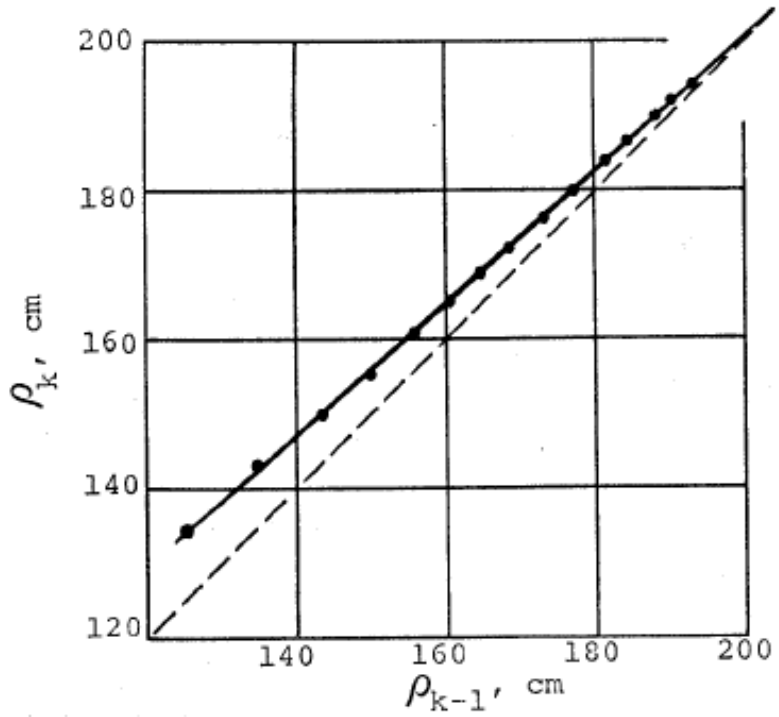

Figure 2.4: Settlement observations ρ_j and ρ_{j-1} (Asaoka, 1978)

The mathematical deduction of Asaoka suggests that the trend line approximating the distribution of the settlement observations will intersect the $x = y$ line in a point that shows the value of the final settlement, ρ_f, since this is given by ρ_j=ρ_{j-1}. Furthermore, the intersection of the same line with the y-axis indicates the value of the β_0 parameter, while β_1 is given by the slope of the trend line.
As mentioned above, Equation 2.12 can be used to predict the settlement value, ρ_j at any time. In fact, by the recursive operation with respect to j, Equation 2.12 yields to (Asaoka, 1978):

$$\rho_{\mathrm{j}} = \frac{\beta_0}{1-\beta_1} - \left(\frac{\beta_0}{1-\beta_1} - \rho_0\right)(\beta_1)^{\mathrm{j}} \tag{2.14}$$

where ρ_0 indicates the initial settlement at $t = 0$. Substituting β_0 and β_1 in Equation 2.14 the settlement ρ_j at any time t_j is known. Another strength of Asaoka's method is that using β_1 retrieved from the previous graph, it is possible to calculate the coefficient of consolidation, c_v using Equation 2.15:

$$c_{\mathrm{v}} = \frac{-4H^2 \ln \beta_1}{\pi^2 \Delta(t)} \tag{2.15}$$

where H is the maximum drainage path and $\Delta(t)$ is the time frame chosen to generate the plot in Figure 2.4. According to Karstunen (2018), c_v values retrieved

using Asaoka's method usually differ by one order of magnitude compared to the ones resulting from laboratory tests, as shown in Table 2.1 below.

Table 2.1: Comparison between c_v values resulting from Asaoka's method and laboratory tests (Karstunen, 2018)

	c_v [m^2/y]		
Site	Lab tests	Asaoka	Ratio
Skå-Edeby	0.16	3.15	20
Penang	0.5	34.7	70
Cubzac B	0.63	6.31	10
Cubzac C	0.44	13.56	31
A-64	2.37	63.07	27
Saint Alban	0.32	2.52	8
R-7	0.20	8.83	47
Matagami	0.25	2.68	10

2.3 Ongoing surface displacement measurements

In Subsections 2.2.2 and 2.2.3 has been introduced how to predict settlement and consolidation and their correlation with time, being it critical for the understanding of the concept. The present study, though, is based on the monitoring of occurring settlement. This section is in fact devoted to the introduction of the different methods used to measure ongoing settlement and to the illustration of their characteristics and differences. The two traditional methods used for the comparison with the InSAR satellite measurements in the present work, and hence the ones introduced in this section, are the optical levelling system and the bellow hose gauge.

2.3.1 Bellow hose gauge

Bellow hose gauges are one of the oldest methods used to measure vertical movements of the soil. Once the tool is in place, the measurement can be done by one man usually in less than half an hour, and they allow to observe both settlement and heave. For these reasons bellow hoses have been widely used in the past and still are today. According to Wager (1973), the installation of the bellow hose involves the positioning of an external casing followed by the one of the hose. The casing, depending on the stiffness of the soil, can be pushed, hammered or drilled down, and is removed after the hose is in place (Wager, 1973). Note that in the specific case of Sweden, the process can result different, with the internal and external cases pushed together in the soil. The quality of the measurement with this tool depends totally on the contact between the soil and the hose, that is why in stiff soils the hole needs to be filled with sand or a thick drilling fluid, while for soft soils, like the present case, the hole usually collapses on the hose creating a proper contact (Wager, 1973).
As stated by Bozozuk and Fellenius (1979), the measuring procedure involves some

metal rings, positioned at predetermined locations in the tube, which are connected to an electric probe attached to a measuring tape. A voltmeter is activated when the probe contacts the metal rings, closing the electric circuit and allowing the measurements, calculated from the top level of the gauge (Bozozuk and Fellenius, 1979). It is important to notice how this method allows to measure soil displacement along the hole vertical and not only on soil's surface.
Wager (1973) explains how the resulting measurements are characterized by an accuracy of plus or minus 2 millimeters. The accuracy is affected by different factors like human reading mistakes, lateral movements of the soil or wrong level surveys. Bozozuk and Fellenius (1979) have though concluded that errors can be reduced if the bellow hose is anchored to bedrock or firm soil that does not move, but this is not always possible.
Figure 2.5 below shows the main components of a traditional bellow hose settlement gauge.

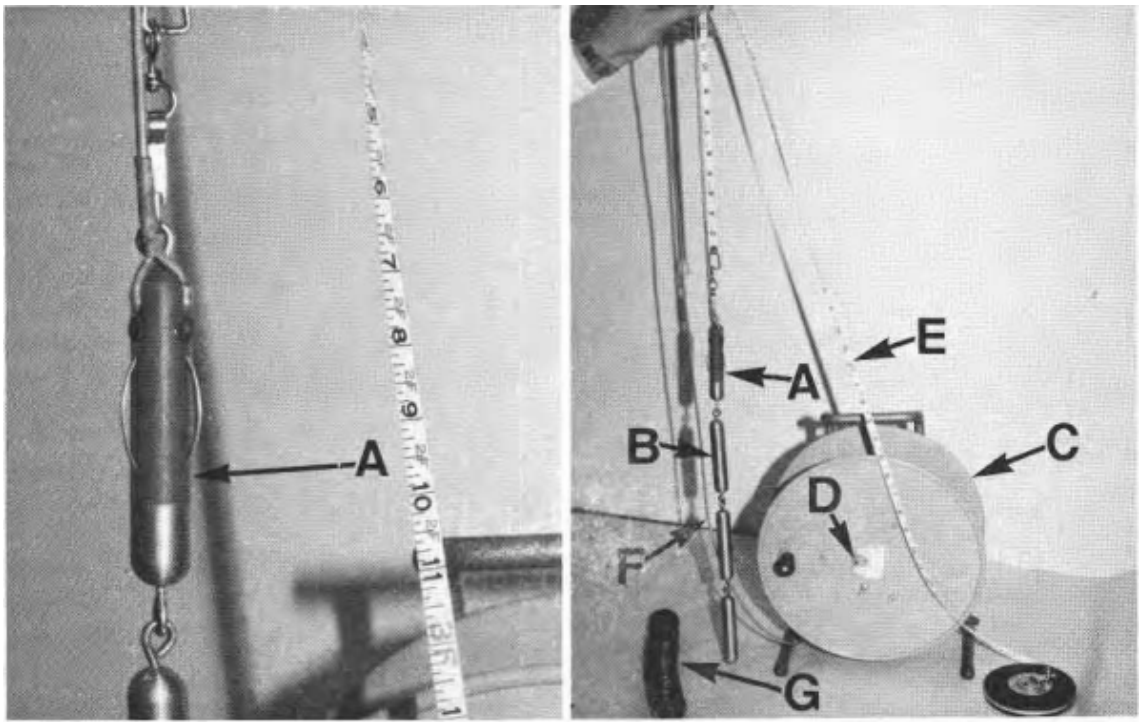

Figure 2.5: Main components of a traditional bellow hose settlement gauge. A: electric probe with flexible spring contacts; B: gauge weights (3x500 g); C: reel; D: voltmeter; E: measuring tape (in inches); F: electric connecting cable; G: sample of axially compressible bellow-hose. (Bozozuk and Fellenius, 1979)

2.3.2 Optical levelling

As well as bellow hose gauges, also the optical levelling system is an old method to measure the displacement of soil surface. The functioning system of this method is based on the retrieving of the height of an unknown point, by the comparison of this to one of known height. This reference point is assumed to have a null vertical displacement over time, hence often positioned on an outcrop of bedrock.

Placing the measuring instrument on the unknown point and looking towards the reference point, it is possible to calculate the height of the unknown point by using the inclination of the instrument and the horizontal distance between the points, to geometrically retrieve the difference in height (vertical distance) between the two points. The process is illustrated in Figure 2.6, where the reference point is in this case represented by a sight on a tripod, but it can also be a stud specifically placed.

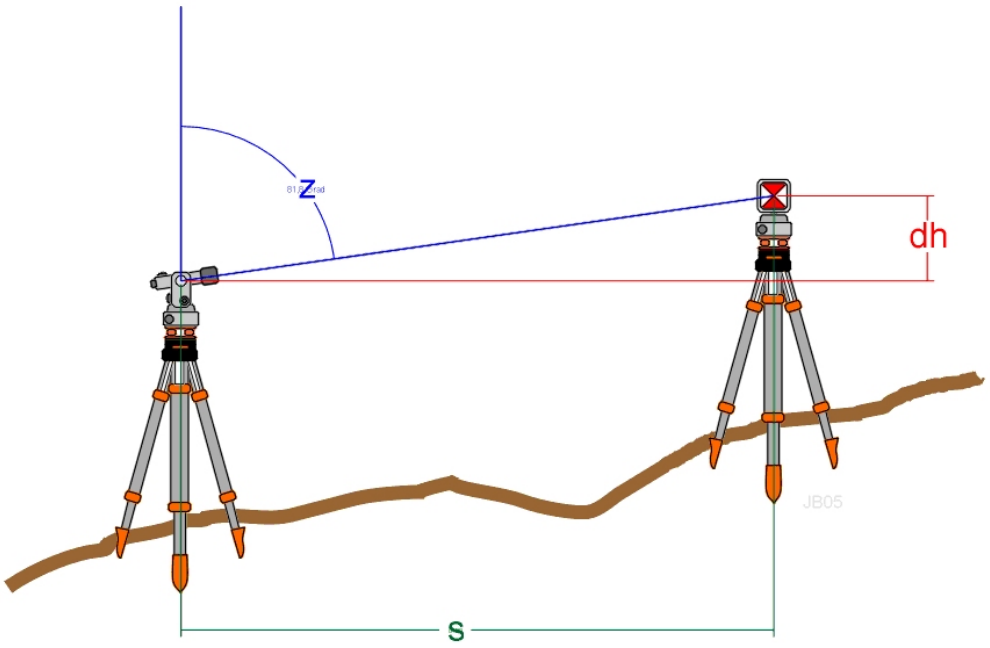

Figure 2.6: Model of optical levelling for surface displacement monitoring. Where 's': horizontal distance; 'dh': vertical distance; 'z': inclination.

The accuracy of the measurements, apart from the quality of the instrument, relies mainly on the distance between the two points, being the error directly proportional to it. For this reason, when is needed to assess the difference in height of a point with great distance from the reference one, the measuring process is iterated as many times as needed to cover the distance maintaining a low error. A way to directly quantify the measuring error is to carry out a close circle of measurements, going back to the starting reference point and assessing its own height resulting at the end of the circle. The difference between the known height and the one resulting from the iteration will give the total error, that can be then split and attributed to each iteration. If carried out properly, this method can guarantee surprisingly high accuracy and precision, reason why it has been widely used in the history of civil engineering, and still is nowadays with modern tools. The application of this method for the assessment of ongoing surface displacement involves measurements of the same point taken a number of times during a time period, using the same reference height. This allows to assess how the difference in height between the two points, hence the surface displacement, behaves during time.

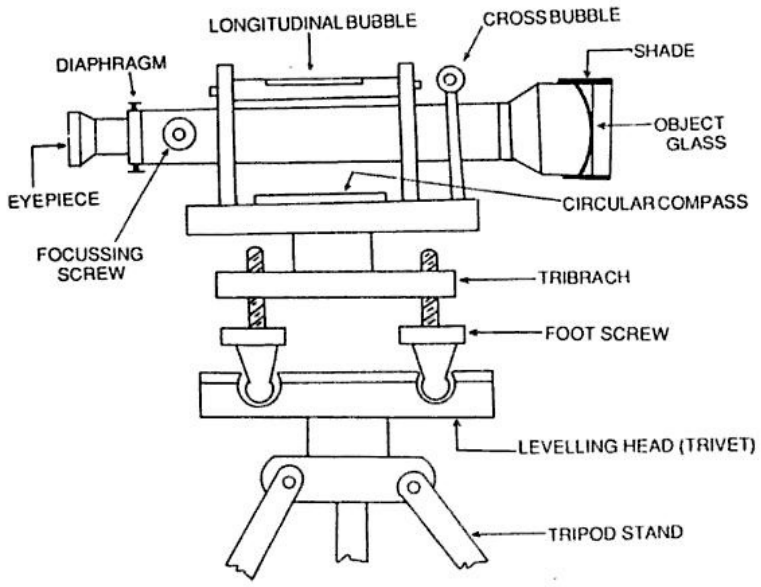

Figure 2.7: Model of a theodolite used for optical levelling

Figure 2.7 illustrates the details of the manual theodolite used to carry out optic levelling measurements. This instrument is assumed to be the one used for the measurements considered in the present work, since they are dated back to 1914. Nowadays also digital, laser or automated theodolites may be found on the market.

2.3.3 InSAR satellite system

As suggested by the present study, the use of commercially available satellite Interferometric Synthetic Aperture Radar (InSAR) techniques, has increased during last years. This is not a surprise since, according to McCormack, Thomas and Solomon (2011), these instruments are capable of remotely mapping and monitoring movements of the soil with an accuracy that goes from meters to millimeters, depending on the context and purpose, without the need to interact with the survey target.

Differently from other satellite systems, like GPS, InSAR system does not need a receiver on site to analyze the signal. In fact, the InSAR radar emits a signal (pulses of electromagnetic radiation) and receives the reflection of it coming form objects in its line of sight. Through an analysis of the signal phase (Figure 2.8), it is then possible to retrieve the distance between the reflecting object and the radar (McCormack, Thomas and Solomon, 2011).

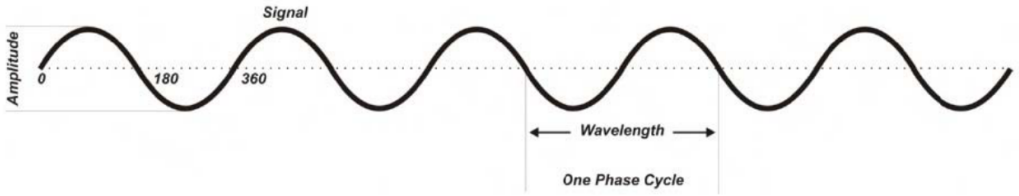

Figure 2.8: Illustration of a radar signal (McCormack, Thomas and Solomon, 2011)

As shown in Figure 2.8, InSAR radar signal can be imagined as a sine wave, characterized by its amplitude and phase. According to McCormack, Thomas and Solomon (2011), the phase of the signal emitted by the radar is known, so it can be compared to the one of the reflected signal, that will be composed by a number of complete wavelengths plus a fraction (the different phase) so to calculate the distance of the object, or in the present case the soil. In other words, if the Earth surface moved towards or away (heave or settlement, respectively) from the radar between the different images, the displacement can be retrieved with an accuracy up to the millimeter from the difference in phase (Bürgmann, Rosen and Fielding, 2000).
InSAR satellites orbit the Earth near the poles, following a latitudinal trajectory (north-to-south or south-to-north) and acquiring images looking at their right, as illustrated in Figure 2.9 below. To retrieve information about the elevation of the target area, a terrain model is used together with many SAR images, taken from the (almost) exact same satellite position, which are combined to produce a radar interferogram (Bürgmann, Rosen and Fielding, 2000). This is then treated and managed through what is called the pre-processing procedure, in order to reduce as much as possible sources of error and to transform raw data in useful information.

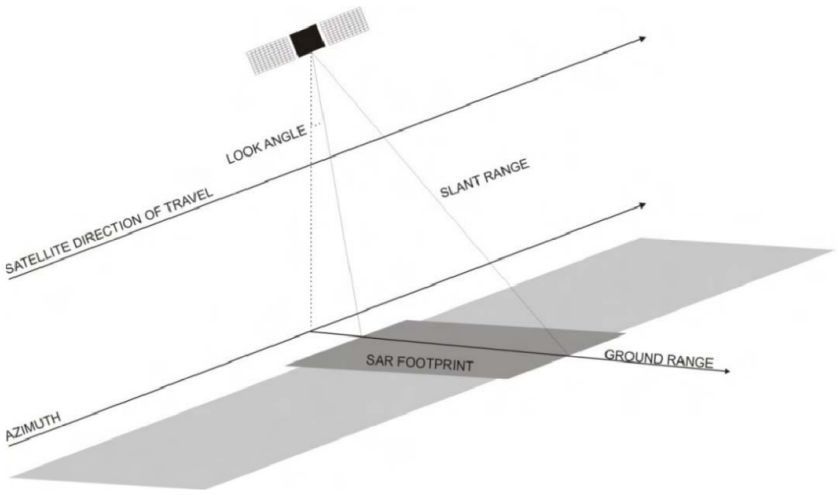

Figure 2.9: Geometry of SAR interferometry imaging (McCormack, Thomas and Solomon, 2011)

InSAR system, as said, can acquire images remotely (often from satellites, but also airplanes or terrestrial platforms) so it does not rely on the conditions (accessibility,

safeness, etc.) of the site. It can work day and night, with any weather condition. It provides images from its archives existing from 1992 (McCormack, Thomas and Solomon, 2011), allowing to compare the behaviour of soil displacement during a wide period of time. It proves to be cost-effective and convenient to use but, despite its numerous advantages, it presents problems as well. The signal emitted by the radar is in fact sensible to disturbance, that can be caused by different factors. Bürgmann, Rosen and Fielding (2000) categorize the possible errors in three classes: phase noise, possibly coming from the radar system, the signal path (the atmospheric water vapor is capable of interfering with the path length) or the processing step; height noise, arising in the mapping process often due to uncertainties in the dimensions of the interferometer; geometric distortion, associated with radar imaging. As explained in details in next chapters, in some geographical areas the measures can also be affected by seasonality, a problem consisting of precipitations that, laying on the soil, reflect the satellite signal before it reaches the soil, leading to a shorter traveling path (hence time) than the correct one.
Note that the term InSAR technically refers to the generation of a terrain model using the phase difference between SAR images, while the retrieving of soil displacement in time is specifically referred to as Differential InSAR (DinSAR). For this work's purposes and simplicity though, the technique will be called InSAR.

2.3.3.1 Sentinel-1 mission

Sentinel-1 represents the first of a total of five missions that the European Space Agency (ESA) is working on for the Copernicus initiative, the European Union's Earth observation programme. This mission includes a constellation of two satellites following a polar-orbit and performing SAR imaging on C-band. They operate day and night and are able to acquire images regardless of the weather. The operation mode characterizing Sentinel-1 is pre-programmed in order to avoid conflicts and to produce a consistent long-term data archive built for applications based on long time series (ESA, 2019). Sentinel-1A, presented in Figure 2.10, is the first of these two satellites and the one from which the measurements used in the present work come.

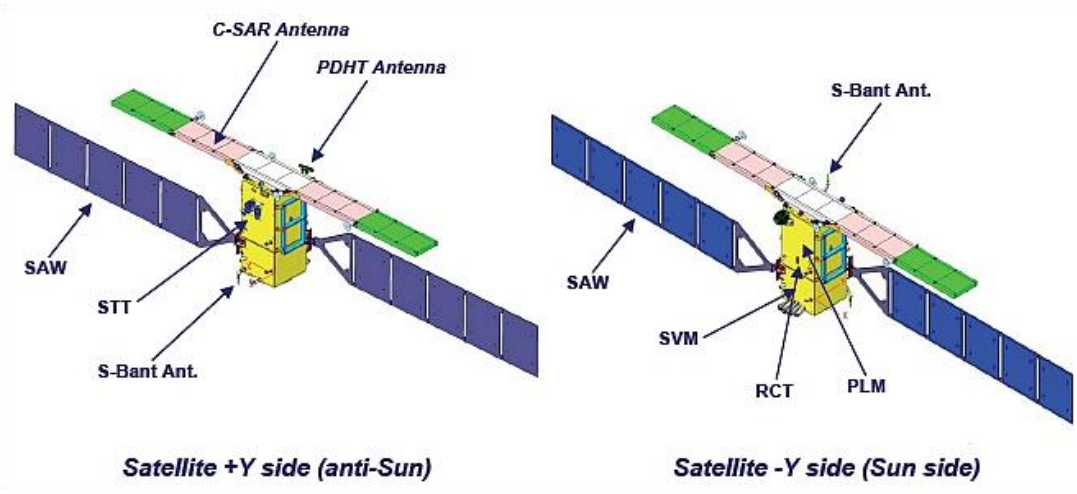

Figure 2.10: Model of satellite Sentinel-1A (ESA, 2019)

Sentinel-1A was launched in orbit on 3 April 2014 and on 6 October 2014 began its operational life, when its data became available to all system users.
The satellite can map the entire world once every 12 days (Figure 2.11), hence the two-satellite constellation guarantees a repeat cycle of 6 days, with a repeat frequency of 1-3 days over Europe (ESA, 2019).

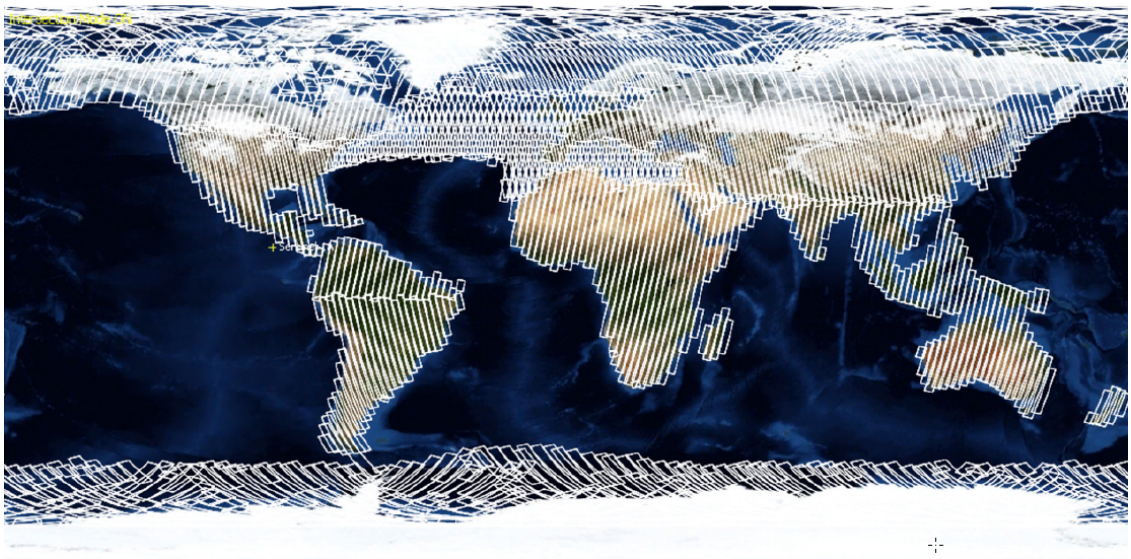

Figure 2.11: Model of a complete world Sentinel-1 SAR coverage (ESA, 2019)

3

Study sites analysis

The very first step for the present Thesis has been the analysis of the different available study sites and the consequential choice of the best fitting ones. This chapter describes how this process has been carried out and which resulted to be the best study sites. Furthermore, the geotechnical and geological past and present conditions of the chosen sites are described in detail.

3.1 Choice of the study site

Five sites have been taken into consideration in total as possible study sites for this work. They are Karlastaden and Frihamnen in the northern part of Gothenburg, Nordstan/Centralen and Masthuggskajen near the city center and the Ajaure dam in the north-western part of Sweden. The availability of a certain study site is intended as the ease and possibility to gather specific data regarding that site, covering all the needed information: InSAR settlement measurements, traditional methods settlement measurements, geotechnical and geological specifics, meaning site and laboratory tests, etc. (as an example look at Figure 3.1).

The InSAR measurements, once pre-processed, come as a wide rectangular area of hundreds points, where each point is characterized by data like vertical rate, mean rate, the single displacement in between each observation, etc. To be able to consider only the InSAR data points of interest, i.e. the ones covering the study sites, the original comma separated value (*csv*) InSAR file has been imported in QGIS software as a delimited text (vector) file. This way, it has then been possible to use the vector clipping tool to select only the InSAR measurement points falling within the areas of interest.

In order to analyse the presence, the type and the magnitude of the detected soil displacement, a further decision-making step was carried out. This was done using the data science capabilities of Python programming, since the size and type of data coming from an interferometric SAR are not practically manageable with Excel. As shown in Figure 3.2 below, using the clipped *csv* InSAR files and their coordinates data, for each site, scatter plots representing data points were overlapped on the correspondent base-map, with the points coloured depending on their mean rate of settlement (or heave, depending on the area).

Figure 3.1: Example of InSAR coverage analysis (black points) for three of the five possible sites: (1)Frihamnen, (2)Nordstan/Centralen, (3)Masthuggskajen.

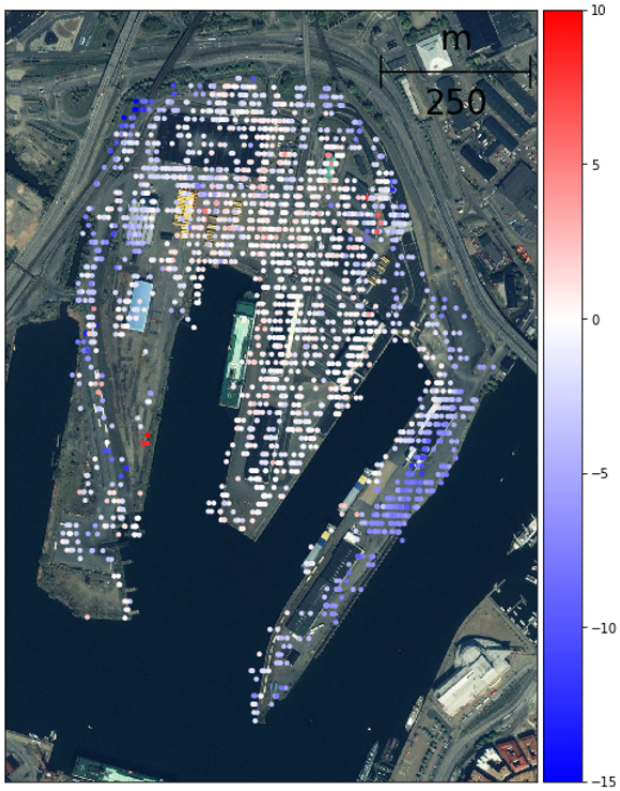

Figure 3.2: Example of displacement analysis for Frihamnen site. Unit: [mm/year]; negative values: settlement; positive values: heave.

Other important factor for the analysis and consequent choice of the study sites has been the availability of company geotechnical data for the areas, coming from specific in situ and/or laboratory tests. Norconsult AB played a fundamental role in this, allowing the use of their reports for the studied areas and making hence possible the retrieving of specific factors needed for the assessment of geotechnical and geological characteristics of the sites, like the coefficient of consolidation, the drainage path length, sub-surface layering and others. In conclusion, through this entire analysis, Frihamnen and Nordstan/Centralen resulted to be the two best fitting sites, hence chosen for the present work. They are presented in detail in the following sections.

3.2 Study site description: Frihamnen

What is today known as the Frihamnen area, around 200 years ago was just a part of Göta river. As can be guessed from Figure 3.3 below in fact, the city of Gothenburg has experienced many artificial dredging and fillings during its recent history. These drastically changed the shape of the river basin, slowly giving birth to the one known today.

Figure 3.3: A map of Gothenburg in 1809

The creation of the new shorelines, that took place in the mid 19th century, consisted of fillings of mud masses, mainly clay, from the river and went on for decades. The northern and southern Frihamnen piers (today know as Norra and Södra Frihamnpiren respectively) were created during the 1910s by dredging the previously completed areas. During 1920-1950, in various steps, the Lundbyhamnen harbor basin and Kvillepiren were successfully created. Lundbyhamnen harbor was taken in use in 1952, when it had a 9 m water depth. In recent years, the water depth has been reduced in the area. Starting in 2011, backfill was added out of Lundbyhamnen's northwestern side and then also the harbor basin has been filled in with clayey mud masses, mainly from the Gothenburg harbor area. Figure 3.4 below can be used as a reference to understand the above description.

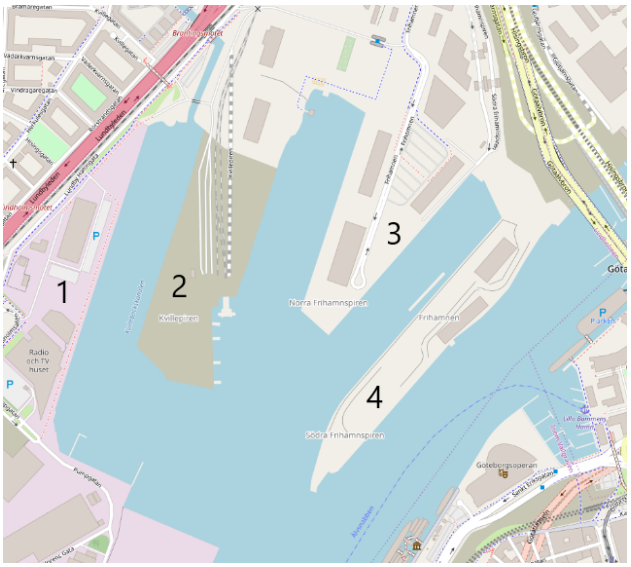

Figure 3.4: A map of Frihamnen area nowadays. [1]Lundbyhamnen; [2]Kvillepiren; [3]Norra Frihamnpiren; [4]Södra Frihamnpiren

The first major quays carried out in the 1910s were characterized by clayey material that was dredged out of them to a certain maximum depth. Then was performed a back-fill with gravel and/or organic material to the expected bottom level and the same material was tilted up towards the center of the pier, creating lateral slopes. Above these slopes the quay decks were built out of wood and were laid out on 15-18 m long wooden piles, as well as a concrete slab which was driven down the quay edge. In the early 1940s, an expansion was carried out to extend to the north-east Norra Frihamnpiren. The quay construction was similar to the one described above, with the exception that no back-fill with friction material was made. Furthermore, a steel wall was installed instead of the concrete slab. In 1964, a new extensive expansion of Frihamnen took place. This expansion meant, among other things, that Kvillepiren channels were filled again and thus, the current inner part created the harbor basin. The quay was constructed with a 20 m deck founded on 40-50 m long wooden piles, length needed to be able to face the load coming from the harbor crane and train. The last expansion in the area was carried out in the early 1970s. A new 20 m wide quay deck made of concrete was built outside the existing quay and was founded on piles driven down in the friction material so to have sufficient carrying capacity to support the design load.

3.2.1 Topography and soil condition

Most of the surface within the Frihamnen area consists of asphalt or gravel. On Kvillepiren, the ground surface is relatively flat with levels mainly varying between +2.0 and +2.5 m. The Frihamnen plan northeast of Kvillepiren has a ground level varying around +2.5 m. Norra Frihamnpiren has similar ground levels, which vary mainly between +2.0 and +2.8 m. The bottom level in Lundbyhamnen varies around -3.0 and -5.0 m, the one of Norra Frihamnpiren varies along the north-west side of the quay edge around -3.0 and -6.0 m and for the south-east and central parts of the harbor base, between -8.0 and -10.0 m. The bottom level of Södra Frihamnpiren

varies from -8.0 to -10.0 m.

The subsurface layering in the area presents three predominant layers on top of the bedrock, being from top filling material (gravel and organic), clay and friction material. The filling material has a thickness of up to about 5 m, found to be higher under Södra Frihamnspiren. The filling materials are generally considered to be contaminated. Under these filling material is found a layer of about 100 m of clay. The clay under the filling soil is made up of a homogeneous "classic Gothenburg clay". The clay density generally varies between approx 1.55-1.65 t/m^3 with a natural water content varying mainly between 0.65-0.80. The clay is classified as intermediate sensitive. There is no deviation in undrained shear strength between the filled clay (the mud masses found in the first meters of this layer) and the homogeneous untouched clay. The undrained shear strength is about 15 kPa at level $\pm$ 0 m and increases with a rate of 0.3 kPa/m. According to performed CRS tests, the clay in the harbor basins is over-consolidated with an OCR of about 2-3. Same tests performed for the shallow clay, show that that it is normally consolidated to slightly over-consolidated, sometimes even "under-consolidated", which indicates ongoing settlements. The bedrock, found to be granite (SGU, 2019), lays at a depth of around 105-115 m.

The measured groundwater head in the upper soil layers of the area is generally around 1-3 m below the ground surface. Levels closest to the quay edges fluctuates around the average water level in the Göta River. These levels for the Göta river in central Gothenburg can be assumed to be the following [m]:

- Highest water level: HHW (50 years) + 1.6
- Normal high water level: HW +1.0
- Normal mean water level: MW +0.1
- Normal low water level: LW -0.6
- Lowest Low Water Level: LLW (50 years) -1.1

The pore water distribution down to approx 15-20 m depth is essentially hydrostatic, based on the average water level in river.

3.3 Study site description: Nordstan/Centralen

Similarly to Frihamnen area, but located on the opposite shore, also Centralen was once part of Göta river, and has been characterized during its history by many changes, as shown in Figure 3.5. Large parts of the area where Central Station lays today is in fact made up of filled and dredged ex water areas.
When the city's fortifications were built in the 17th century, the shoreline used to lay just north and east of what is Nordstan nowadays (Figure 3.5). During the mid-1800s, the area Gullbergsvass was dredged and filled out. New soil was also filled between the fortifications and Hultman's islets again during this period, leading towards the shape known today.

Figure 3.5: History of Nordstan/Centralen area. [1] 1820; [2] 1860; [3] 1890; [4] 1921 (map from 1790 in background)

3.3.1 Topography and soil condition

The soil layers underneath the area's surface consist of filling material and a naturally deposited layer of clay to a great depth that rests on friction soil, above bedrock. The filling material thicknesses are generally around 2.5-3.0 m. This material is commonly at the top of about 1.0-2.0 m of a mixed layer characterized by stones, gravel, sand, paving stones and demolition remains originating from the 20th century. Below, fine-grained materials such as sand, silt and clay follow with bricks, wood and glass remains (derived from mud and shaft masses from 19th century) as well as basic remains from previous construction works. Organic soil is also present in this layer. Below these first meters, a naturally deposited clay follows to a great depth. Cone penetration test (CPT) investigations performed in the area show a homogeneous clay without any occurrence of draining / water-bearing layers. Same tests show the clay reaching a depth around 85.0-100.0 m within most of the station area. Under the clay, a layer of friction soil (not closer examined) that rests on the

bedrock follows, with bedrock at an approximate depth of 85.0-100.0 m and mainly consisting of granite (SGU, 2019).

Geotechnical parameters characterizing the clay are a density of about 1.6 t/m^3 down to -18.0 m, that increases to about 1.7 t/m^3 below the depth of 60.0 m. Furthermore, its water content varies around 0.60-0.90, with the higher values found down to depth of about 10 m. The clay is intermediate sensitive with a sensitivity that generally varies between 10 and 30. It presents on average an undrained shear strength of 15 kPa down to -3 m that increases with depth with a rate of 1.6 kPa/m. The clay is in general over-consolidated, with the OCR going from 1.4 at around -3.0 m to 1.3 at a depth of around -50.0 m.

Groundwater is found partly in the superficial filling material layers, and partly in the friction material layers under the clay. Measurements in the upper reservoir shows that the groundwater head is at +0.5 to + 1.5 m. The proximity to the Göta river leads to the groundwater level in the upper reservoir being dependent on the water level in the river. Both recent and old pore pressure measurements show that the pore pressure level in the clay corresponds to a groundwater head that is at +0.5 m. Measurement at greater depth shows, on the contrary, higher pressure levels, indicating a tendency to over-pressure (pressure levels corresponding to a higher groundwater head of about +1 to +4 m).

4

Methods

In the present chapter the reader will be presented with a detailed description of all the methodologies used for accomplishing the totalities of aims and objectives of this Thesis study. The chapter is divided in sections, each of them devoted to the explanation of the work process used for the single bullet points presented in the introductory Section 1.2. None of the results achieved through the methodologies presented will be shown in the present chapter, for those, please refer to the following one.

4.1 InSAR and traditional measurements comparison - Nordstan

The traditional settlement measures available in Nordstan/Centralen site came from bellow hose gauges. Settlement measurements coming from bellow hose gauges and the ones deriving from interferometric SAR system, are conceptually and technically different. As previously explained, bellow hose gauges measure settlement along the vertical of a specific point, returning the behaviour of the displacement of the soil with depth. In this case in fact, the resulting measurements consist of a total settlement value for each of the depths analyzed by the gauge (refer to Subsection 2.3.1 for more details), where measurements are taken on different dates, with no fixed time pattern. So the data represents the total settlement in that point (position of the gauge), for a depth of interest, on a certain date. On the other hand, InSAR data give, according to their operation (refer to Subsection 2.3.3), the difference in height of the soil's surface between a 0-time image, taken as the reference height, and the other images, all often taken 12 days apart from each other. Hence, comparing two such different measuring methodologies can not be so immediate, given the two main issues of time (dates) and space (depth) differences.

For the present study, the comparison has been divided in different, modular steps and structured as follows. The steps represent different comparing approaches, that go from less to more detailed, to give an idea about the relations between data science methodologies and consequential results.

4.1.1 Comparison based on rate of displacement, single point

For this comparing step, the measures data coming from a specific bellow hose gauge (C in Figure 4.5) has been compared to the ones resulting from a single InSAR point in the exact same position (ID:821). First of all, since the InSAR measures are related to the soil's surface, only the most shallow measures (surface proximity) from bellow hose gauges have been considered. Second, the dates corresponding to the measurements have been turned to days, to have a consistent and continuous time axis.
The plot in Figure 4.1 below shows this step, where the points are the single measurements, simply linked by straight lines. Such an interpolation though is definitely not accurate enough, since to compare these data to the InSAR ones the need was to have reliable settlement values with a temporal cadence of around 12 days (as said, time span for images acquisition with SAR).

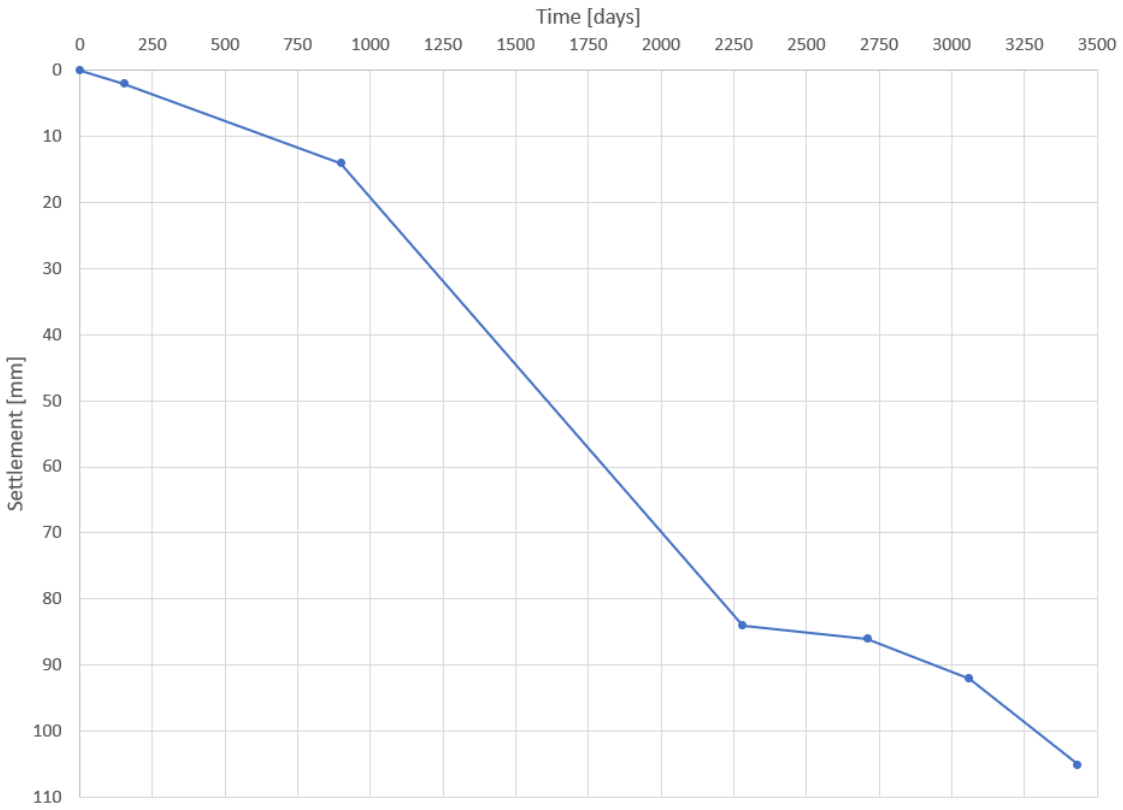

Figure 4.1: Surface settlement from bellow hose gauges measures

The data have been hence properly interpolated using Python, using a 6^{th} order polynomial that resulted in more than 270 interpolated values between the real points. The resulting plot is presented in Figure 4.2 below.
The last step to make the comparison possible has been to use the concept of rate of settlement, r, taking into consideration the same time span, of 12 days.

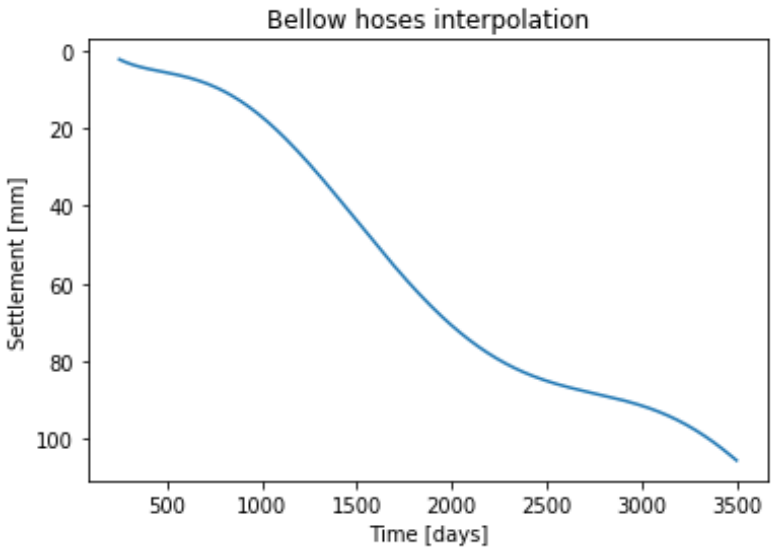

Figure 4.2: Surface settlement 6^{th} order polynomial from bellow hose gauges measures interpolated using Python

For the bellow hose gauges data, Equation 4.1 was used since every value represented the total settlement in that moment:

$$r_{\text{bhg}} = \frac{s_{\text{i+1}} - s_i}{t_{\text{i+1}} - t_i} = \frac{s_{\text{i+1}} - s_i}{12days} \tag{4.1}$$

where s_i is settlement at step i and t_i is time at same step. On the other hand, being the SAR data a vertical displacement with respect to the reference height, the formula used for the rate, r, was:

$$r_{\text{SAR}} = \frac{d_{\text{i+1}} - d_i}{t_{\text{i+1}} - t_i} \simeq \frac{d_{\text{i+1}} - d_i}{12days} \tag{4.2}$$

where d_i is vertical displacement between image i and reference height and t_i is time at step i. Note that in this case the value of vertical displacement can be both settlement or heave, being the InSAR sensible to all surface height changes (seasonal variations) so r represents the rate of displacement more in general. Only the negative values of r will indicate settlement, while the positive heave.
As some will have noticed, Equation 4.1 and 4.2 differ by the 'equal' sign characterizing the last step of the equations. This is because the values in Equation 4.1 are interpolated ones, hence they all differ by 12 days, while the ones in Equation 4.2 are real values, thus some of them are missing or not respecting the temporal difference of 12 days.

4.1.2 Comparison based on data-set trend-line, single point

Using the same bellow hose gauge data and the same correspondent InSAR point, measures have been compared plotting the values against time and using trend-lines to determine an average behaviour. The unit chosen to do so consisted of millimeters of displacement per year [mm/year], related always to the soil's surface only.

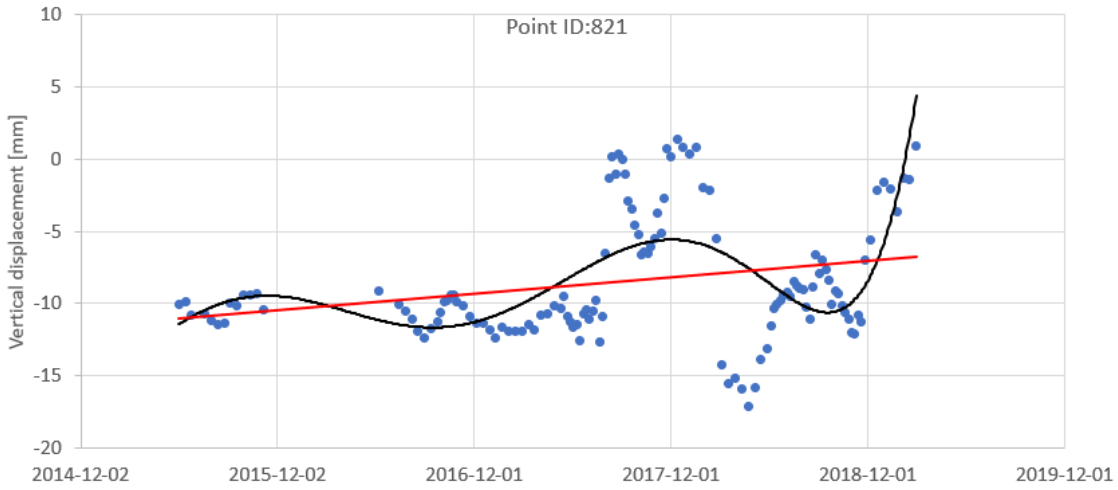

Figure 4.3: InSAR point (ID: 821) measures against time, showing averaging function (black) and trend-line (red)

As shown in Figure 4.3 above, where the measures are from the SAR point (ID: 821) correspondent with the bellow hose gauge C, the x-axis that represents time consists of dates, being them the ones on which each SAR image has been taken. It is also visible that for this InSAR data-set, the reference height taken as 0-time is found to be the one imaged on 2017-09-01, being its value equal to zero. Figure 4.3 illustrates how InSAR data are subject to noise and fluctuations, reason why their behaviour is studied through the use of trend-lines and functions averaging the data, that are the linear and polynomial functions in the figure, respectively.

One of the methods used to assess the fluctuations of InSAR data is to analyse possible seasonality of the measurements. As previously mentioned, the signal emitted by Sentinel-1A satellite is reflected by the first object found on its path, it is hence impossible for the satellite to determine if what reflected the signal was the soil surface or just a temporal snow coverage. This can lead to significant fluctuations in the resulting measures, that, if not recognized, could consequently be reason for mistaken interpretations of data. Think for example of a snowy winter characterized by consistent 10/15 cm precipitations. From the raw data, this could be misinterpreted as a 10/15 cm heave of the soil developed in a single season, something definitely not common. This fact could not represent a problem for some warm climate countries, but surely does in a Scandinavian city like Gothenburg.

In order to avoid fluctuations of this type related to seasonality, data have been filtered with respect to the specific season in which the images have been taken. A first more simplistic step, consisted of removing all the measurements taken during winter: a new plot has been created, that took into consideration all data correspondent to dates between March the 15th and November the 15th.
Limitations of this method lay in the fact that even a cold city like Gothenburg is not always characterized by snowy winters. Furthermore, when it does, not every single winter day can be assumed to be snowy. For this reason, a second, more precise and detailed filtering of data has been carried out. This time, the dates of

the InSAR images have been selected with respect to the average temperature of the single days. In fact, on the website of the Swedish Meteorological and Hydrological Institute (SMHI, 2019), such information, and other of this kind, are publicly available for downloading and/or consultation. It has been assumed that snow could be found during winter days characterized by an average temperature lower than 2 °C, hence the new plot has been created including only data imaged on days with an average temperature higher than 2 °C.

Plots similar to the one in Figure 4.3 have been created for all the three cases described above (full year - no winter days - no snowy days). The trend-lines approximating the three InSAR data plots, have been all compared to the same trend-line resulting from the plot of the interpolated bellow hose gauge C data, since its measures are not affected by seasonality.

4.1.3 Comparison based on data-set trend-line, groups of points

Not all InSAR data points are equally reliable. Disturbance (noise) varies between each point, an approach that consider group of points more than a single point is therefore argued to be more reliable. For example, the data point (ID: 821) considered in the previous two subsections, presents a temporal coherence equal to 0.57, where the overall coherence average in this area lays around 0.7, proof of the fact that possibly that does not represent the best approach. For this reason, a different and more specific comparison approach was used, consisting of studying the InSAR data points with regards to their trend, looking for areas where close points had a similar trend, as much as possible next to areas of interest, them being bellow hose gauges positions.

More specifically, similarly to the process adopted during the choice of the best study site, the data has been plotted on a base-map and coloured according to their trend (rate and type of vertical displacement) so to be able to address areas of points with similar trends (Figure 4.4).

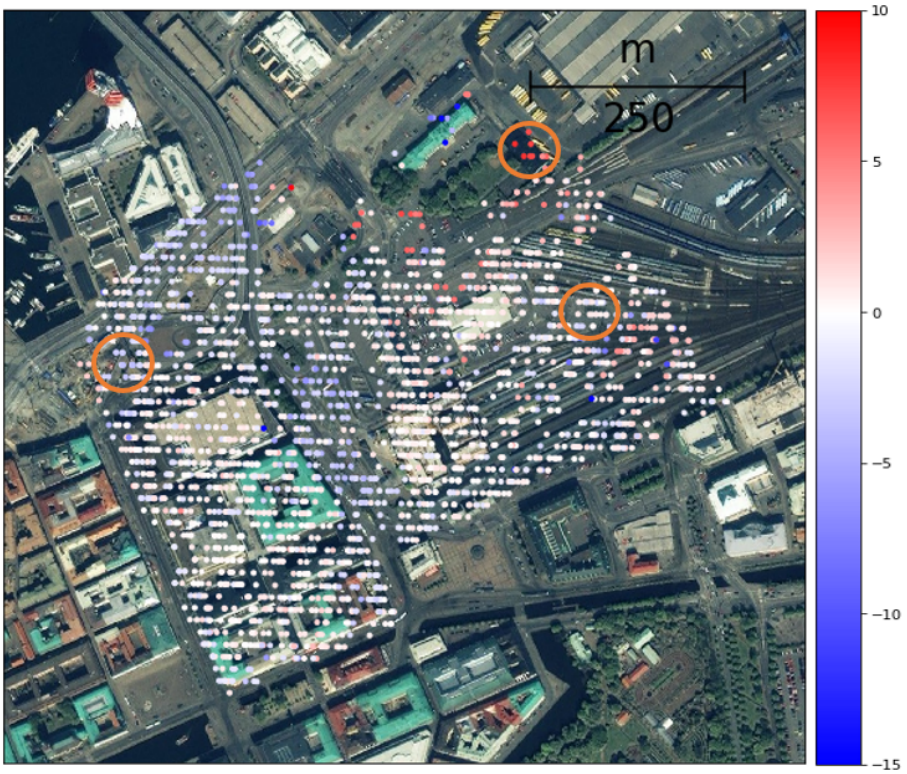

Figure 4.4: Trend of InSAR points for Nordstan area. Legend: unit is [mm/year] and negative values mean settlement

Looking at the areas in proximity of the three available bellow hose gauges, presented in Figure 4.5, it was possible to identify three main zones with consistent and similar trends (orange circles in Figure 4.4), each one including 6 or 7 data points.

Figure 4.5: Bellow hose gauges positions in Nordstan area

For each group of points, the data have been extrapolated and plotted together on the same displacement-time graph (Figure 4.6). A trend-line has been used to

summarize the behaviour of each of the single data points. In the end, the average of these trend-lines has been used to indicate the vertical displacement mean velocity for each of the three orange circles in Figure 4.4, and compared to the one measured by the correspondent bellow hose gauges.

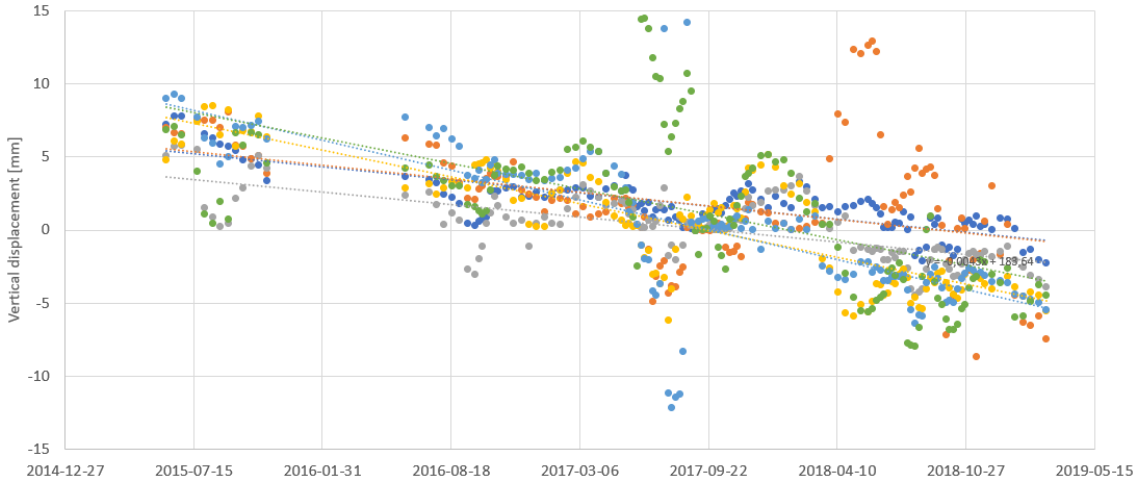

Figure 4.6: Example of vertical displacement trend for the group of InSAR points around bellow hose gauge A

The same reasoning done in Subsection 4.1.2 about the seasonality of InSAR data, is consequentially valid in the case of trend areas too. In fact, this is clearly visible in Figure 4.6, where is shown how the values between January and March 2017 and between November 2017 and February 2018 deviate from the average trend, being higher. For this reason, also in this case the data have been filtered removing the winter dates measurements.

4.2 InSAR and traditional measurements comparison - Frihamnen

The traditional settlement measures available in Frihamnen site came from optical levelling. This kind of measures are more similar to InSAR compared to bellow hose gauges, since they show the settlement of the soil surface. This allowed for a more direct comparison between the two, that started from the data plots available from optical levelling (presented in Appendix A due to their size, Figure A.1 and A.2). From these plots, one with the measures from Norra Frihamnspiren and the other from Södra Frihamnspiren, the mean behaviour has been retrieved extracting the data of three points resembling the average trend. These points have been plotted on a new graph, showing the trend line and its coefficient of determination, R^2, for each (Figure 4.7). To make the comparison with InSAR data more accurate, the InSAR data points available for the Frihamnen area have been grouped using QGIS, in two areas, one for Norra Frihamnspiren and one for Södra Frihamnspiren.

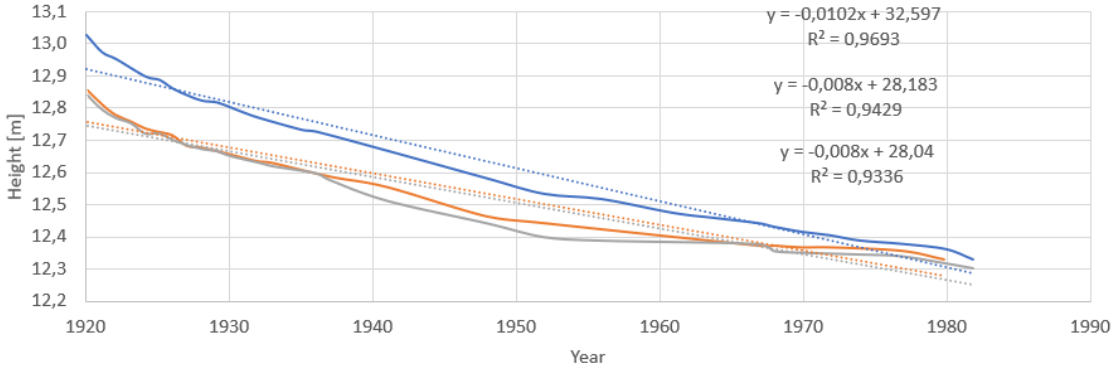

Figure 4.7: Example of vertical displacement trend for the 3 optical levelling data points representing Södra Frihamnspiren

The average vertical displacement of the soil resulting from this InSAR analysis, has been compared to the one coming from the last optical levelling graphs, where these last have been weighted depending on their R^2 values.

4.3 Settlement hand calculation

The comparison between traditional and InSAR measurement methods previously discussed, allows to highlight analogies and differences between the two, relating the vertical displacement of the soil to a more extended time frame, based on all the methods (this will be further discussed in Chapter 6). In order to have a broader and more complete vision of the analysis, and to asses potential usefulness of them, the InSAR measurements have been also used as a starting basis for the prediction of future settlement values. The method chosen to do so is Asaoka's "observational procedure" (the method is explained in details in Subsection 2.2.3).

Two locations have been selected for such analysis, one for each study site. Since Asaoka's method is based on soil settlement measurements, so not on soil vertical displacement measurements in general, the InSAR data coming from the selected points have been filtered depending on the displacement measured by them. In fact, as previously discussed, InSAR measures can fluctuate consistently because of a number of reasons (seasonality, reflection noise, etc.), so even measures coming from a high quality data point won't appear as the usual consistent settlement measurements one is used to see (example in Figure 2.3). For this reason, filtering the data was needed and to do so both the data points groups have been represented by an average trend of single date measures, based on all the measures resulting for that date. Then, only the dates showing settlement, hence a vertical displacement lower than its previous one, have been selected. This because InSAR shows the vertical displacement relative to a certain date and not the absolute one, as previously explained. Now, having only the relative settlement measures, was possible to add them up to have the absolute settlement values for each date, somehow similar to usual plots as Figure 2.3. These absolute values were plotted, as explained in Subsection 2.2.3, against each other, to create graphs like the one in Figure 4.8.

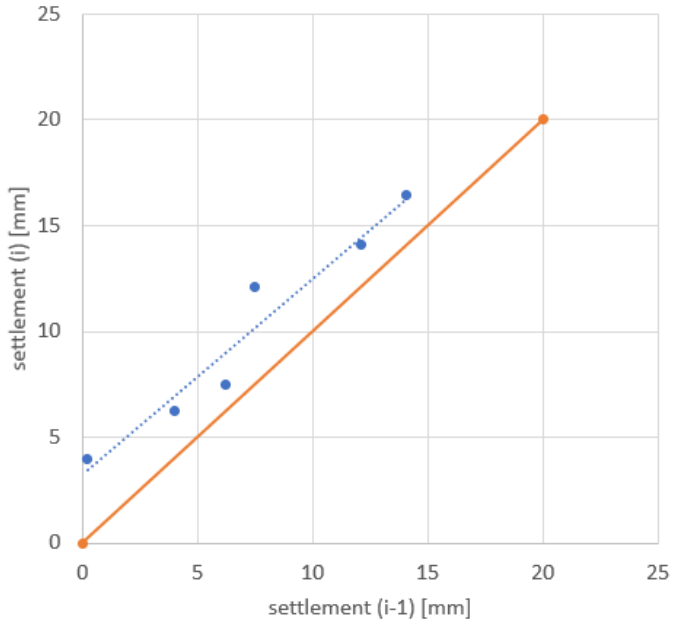

Figure 4.8: Resulting Asaoka's plot coming from InSAR measures in Södra Frihamnspiren, Frihamnen site

Through these procedures, was possible to forecast the final settlement values for the areas based on the InSAR measurements. Furthermore, using Formula 2.15 it was possible to retrieve the values of the coefficients of consolidation, used after for the discussion about usefulness and characteristics of this kind of measurements.

4.4 Analysis of InSAR uncertainties and statistical parameters

When it comes to establish the goodness and usefulness of a measurement method, its reliability and accuracy play a primary role. In the present section is explained how the available interferometric SAR data have been analyzed and how these factors have been studied. Furthermore, a comparison has been carried out between the different resulting satellite measures when considering different classes of data points depending on the consistency of their measurements. The entirety of the present section's analysis was carried out using Python data-science capacities, given the size of this data (thousands of points with hundreds of measurements each). Precisely, a specific Python code was developed, written and used in order to operate with such an amount of data. The code is reported in Appendix B.

As introduced in previous sections, an InSAR measures data-set can be imaged as a matrix, where the rows are the data points and the columns are a series of information (characteristics, position of satellite, soil displacement measures, etc.) related to the point. In order to make the understanding of this analysis smoother, imagine this matrix composed by soil displacement measures only, hence rows corresponding to data points (thousands) and columns showing the measured soil displacement on

each different date (hundreds) for each point. This is exactly what the first part of the code does: it extracts the measures from the entire InSAR file. After that, the code:

- creates a list of n arrays (vectors) containing the displacement measures, where n is the number of data points
- creates one array with the dates on which the measures were taken (common to the entire data-set)
- generates n scatter plots using the n displacement measures arrays as y-axis and the dates array as x-axis
- draws a linear trend-line for each plot
- calculates the coefficient of determination, R^2 and the slope of each trend-line
- extrapolates three groups of points, according to the three conditions R^2>0.5, R^2>0.75 and R^2>0.9
- calculates the number of points in each group and the median of their displacement trends (in mm/year)
- plots the data points on a base map, highlighting the ones with R^2>0.75

This analysis method is referred to as linear regression and is one of the most widely used statistical method to assess one data-set's quality and consistency. The three conditions R^2>0.5, R^2>0.75 and R^2>0.9 were respectively chosen to filter out the very bad quality points (not usable), select a larger class of higher quality points and select a smaller class of highest quality points.
The code was written in such a way that it could be used for all the InSAR data-sets, hence the same procedure explained above was applied to every study site's InSAR data-set, using the same code.

Since it is interesting and useful not only to calculate numerical results but also to visualize the findings, especially when analysing data that relate directly to space, the two higher quality classes of points (so all the ones with R^2>0.75) have been plotted on a base-map for both the study sites, so to assess a possible pattern in their position and study their distribution. This allowed to compare the data coverage before, so using the entire data-set and after, so using only more reliable data points, in order to compare the size scale of traditional geotechnical information with InSAR one. In conclusion, an assessment of how the density of data points varies when considering the different quality classes has been carried out. Again, the analysis was done using Python and the results are shown both in a numerical (average density table) and a visual way (heat-maps).

5
Results

The present chapter will illustrate and explain all the findings that the single steps of this study achieved. To follow a structure similar to the one of the previous chapter for the methods, the results are presented in different sections, that follow the original division of the initial objectives and aims.

5.1 InSAR and traditional measurements comparison - Nordstan

As seen, the comparison for this study site has been carried out using three different methods and compared InSAR data to bellow hose gauges. The InSAR data-set covers the period between 2015-06-02 and 2019-03-01 while gauges measures are less recent, covering the period from 2005-05-11 to 2016-09-15. Tables 5.1, 5.2 and 5.3 below illustrate the results for rate of displacement for a single point, average trend for a single point and average trend for group of points respectively, where the negative values of vertical displacement indicate settlement and the positive heave.

Table 5.1: Comparison based on rate of displacement, single point

Measure	Rate [mm/y]
Bellow hose gauge C	-11.6
InSAR point (ID:821)	+6.7

Table 5.1 clearly shows how inaccurate results can be if only a single InSAR point is used as reference. In fact, bellow hose gauge C suggests a consistent settlement of the soil's surface in that point with 11.6 mm each year, while the correspondent InSAR point not only does not indicate settlement, it actually suggests a tangible heave of 6.7 mm per year.

Table 5.2: Comparison based on data-set trend-line, single point

	Trend [mm/y]		
Measure	entire year	no winters	no snowy days
Bellow hose gauge C	-13.1	-	-
InSAR point (ID:821)	+1.2	+0.2	+0.6

From Table 5.2 two facts can be observed. First, same data can give different results depending on how they are analyzed. In fact, the same bellow hose gauge indicates a rate of displacement (Table 5.1) that differs from its average trend (Table 5.2) by 1.5 mm/year, same is valid for the InSAR point, where the difference consists of 5.5 mm/year. Second, a confirm of how seasonality affects interferometric SAR data. Removing the measurements taken during winter, the resulting trend differs in fact by 1 mm/year from the one related to the entire year, indicating a soil vertical displacement proximate to zero. This value is more reliable and can be considered slightly more precise of what it appears, despite the difference with the one from the gauge, when taking into consideration the reflections presented below in the discussion chapter, related to the distance in time of the measures, introduced above, and surrounding environment. On the other hand, less difference is seen between the result obtained removing all the winters or only the days assumed to be snowy, based on their temperatures.

Table 5.3: Comparison based on data-set trend-line, groups of points

		Trend [mm/y]	
Area	Measure	entire year	no winters
A	Bellow hose gauge	no data	-
A	InSAR points	-2.5	-2.6
B	Bellow hose gauge	-13.2	-
B	InSAR points	+7.4	+7.0
C	Bellow hose gauge	-13.1	-
C	InSAR points	-0.1	-0.2

In conclusion, Table 5.3 proofs that taking into consideration InSAR trend areas more than single points gives more precise results, showing, for area C, a behaviour finally consistent with the gauge's one, settlement. The difference in magnitude is, as said, further discussed in next chapter. When it comes to area B, a strong deviation of InSAR measurement from gauge's ones is seen, both excluding data seasonality and not. Area A results the only one to be characterized by a tangible InSAR suggested settlement, but unfortunately the data coming from its bellow hose gauge were not available, so no comparison was possible.

5.2 InSAR and traditional measurements comparison - Frihamnen

When it comes to Frihamnen study site, the InSAR data were compared to optical levelling ones, and the comparison was carried out separately for the two piers Norra and Södra Frihamnspiren. This was possible thanks to data availability and assumed to be more accurate. The InSAR data-set in this case covered the same period (2015-06-02 to 2019-03-01), but the measures from optical levelling are older, spread on a longer period going from 1914 to around 1988. The findings are pre-

sented in the following table.

Table 5.4: Comparison based on data-set trend-line, groups of points (Frihamnen)

	Trend [mm/y]	
Measure	Norra Frihamnspiren	Södra Frihamnspiren
Optical levelling	-2.1	-8.7
InSAR points	+0.1	-4.7

Table 5.4 shows how in this case the results of the comparison are more consistent. InSAR measurements in fact, differ only by 2.2 and 4 mm/year from optical levelling ones for Norra and Södra Frihamnspiren respectively. One more time, in the next chapter will be discussed why such results should be looked at as more precise and similar than what they look.

5.3 Settlement hand calculation

Asaoka's "observational procedure" was used to predict the surface settlement behaviour in both the study sites, starting from InSAR displacement measurements. Södra Frihamnspiren and area A have been chosen for Frihamnen and Nordstan respectively for the present analysis, because as seen in previous sections they are the areas characterized by a higher settlement, fact that makes their choice more interesting for this study's purposes. The results of the procedure are illustrated below.

Table 5.5: Settlement prediction results for both study sites

Area	β_0	β_1	s_{100} [mm]	c_v [cm^2/s]
Sodra Frihamnspiren	3.26	0.92	43	0.046
Nordstan area A	1.95	0.97	75	0.012

According to Table 5.5, the value of the final settlement for Södra Frihamnspiren is expected to be 43 mm, while the one for area A in Nordstan lays around 75 mm. Comparing these findings to the ones of previous sections, it is straightforward to conclude that, according to these results, in Sodra Frihamnspiren the total settlement takes around 10 years to be reached, while the one in area A Nordstan takes around 28 years. These periods of time have not to be intended from today, but from when the InSAR data-sets of measures for this areas respectively start. Furthermore, the settlement of soil in these sites is an on-going process, extremely complex to model. It did not start together with InSAR measurements of course, so 10 and 28 years are not times needed to go from 0 to 100 % of settlement, but to go from what was the state of settlement at the time of the first InSAR measure, to its final value of consolidation (not including creep). These concepts will be further discussed in the following chapter.

When it comes to the coefficient of consolidation, Table 5.5 shows that the one characterizing Frihamnen area is almost four times bigger than the one resulting for Nordstan area, hence an opposite trend compared to the one of respective final settlement. This could find its reason in the pore water drainage path length, H, a parameter used in Formula 2.15 as squared, thus heavier than others. It is worth mentioning how this value, for both study sites, is quite approximate, laying in a range of 10-15 m (8-10 %) of uncertainty, consequentially leading to a grade of uncertainty for c_v as well. Nevertheless, the available results from CRS tests carried out for Nordstan area suggest an average c_v that lays around 0.001 cm^2/s, hence differing by one order of magnitude from the one presented above, perfectly agreeing with Table 2.1 presented in the literature review.

5.4 Analysis of InSAR statistical parameters

In order to assess the statistical quality of the available InSAR data-sets, a specific Python code has been developed. The aim was to carry out a linear regression analysis to see how reliable these data are and consequentially the results, based on their behaviour over time. The code was used to analyze all the data-sets object of the present work's assessment and the findings are presented below. The R^2 gives an idea of how consistent in time the behaviour of the soil is, according to each point. So dividing the points according to this parameter is a simple but effective method to sort out higher quality data points, and give more consideration to their measures.

Table 5.6: Statistical parameters of InSAR data-set Nordstan/Centralen

Class	N of points	% of total	Median trend [mm/year]
R^2>0.50	335	13.8	-2.57
R^2>0.75	86	3.5	-4.33
R^2>0.90	8	0.3	-15.06

Looking at Tables 5.6 and 5.7, it is easily noticeable that both Nordstan and Frihamnen data-sets are not in general characterized by many high quality data points. In fact, they respectively result to have more than 80% and 70% of points with high fluctuation and consequent unreliability (R^2<0.50). Another evident fact is that the magnitude of the median settlement of each class of points is directly proportional to the class' R^2 value. This is explained by the fact that seasonality and reflection noise normally lead to a shorter traveling path for the satellite signal, hence a mistaken soil surface higher than the actual one.

Table 5.7: Statistical parameters of entire InSAR data-set Frihamnen

Class	N of points	% of total	Median trend [mm/year]
R^2>0.50	657	27.6	-4.78
R^2>0.75	341	14.3	-6.44
R^2>0.90	106	4.4	-7.12

As shown in Tables 5.8 and 5.9 below, from Frihamnen data-set the two data-sets for Södra and Norra Frihamnspiren have been in turn extracted and analyzed, so to assess these aspects on a more detailed scale. On the one hand, the first shows remarkable quality points, with almost four fifths of them with a R^2>0.50 and over 20% of them laying in the top class.

Table 5.8: Statistical parameters of InSAR data-set Frihamnen cut, Södra Frihamnspiren

Class	N of points	% of total	Median trend [mm/year]
R^2>0.50	257	72	-6.26
R^2>0.75	191	53.5	-6.67
R^2>0.90	75	21	-6.89

On the contrary, the second is characterized by an extremely low temporal coherence, with only 1.5% of points in the R^2>0.50 class and the other two completely empty. This fact proves that within a single InSAR data-set both high and low reliability areas can be found and that data quality is not equally geographically spread.

Table 5.9: Statistical parameters of InSAR data-set Frihamnen cut, Norra Frihamnspiren

Class	N of points	% of total	Median trend [mm/year]
R^2>0.50	8	1.5	-2.22
R^2>0.75	0	0	-
R^2>0.90	0	0	-

Now that low quality/reliability points have been removed from the data-sets, a new comparison with the measures coming from traditional methods is possible. Going back to Tables 5.3 and 5.4 for Nordstan bellow hose gauges and Frihamnen optical levelling respectively, it is interesting to notice how similar to these values InSAR ones are now (Table 5.10), with due care.

Table 5.10: Comparison between InSAR quality points (R^2>0.90) and traditional methods

	Trend [mm/y]		
Measure	Nordstan	Norra Frihamnspiren	Södra Frihamnspiren
Optical levelling	-	-2.1	-8.7
Bellow hose gauges	-13.1	-	-
InSAR quality points	-10	-1	-7

Considering that the R^2>0.90 class can be seen as the most reliable only depending on how many points it includes (8 points are not enough), it is possible to conclude that the most realistic settlement trend resulting from Table 5.6 will be lower than -15 mm/year. Given the direct proportionality between the parameters mentioned above, this settlement trend can be assumed to lay around -10 mm/year, resulting consistent with the -13 mm/year agreed by both the bellow hose gauges in Table 5.3. Furthermore, Table 5.8 shows that 75 reliable points suggest a settlement trend of around -7 mm/year for Södra Frihamnspiren, value proximate to the -8.7 mm/year resulting from levelling measures in Table 5.4. In conclusion, when it comes to Norra Frihamnspiren, it is possible to combine Table 5.5 (full data-set) and 5.9 (8 higher quality points) to conclude that the most realistic trend will fall within the gap in between them (+0.1 and -2.2 mm/year) resulting again really similar to levelling measures, that suggest -2.1 mm/year.

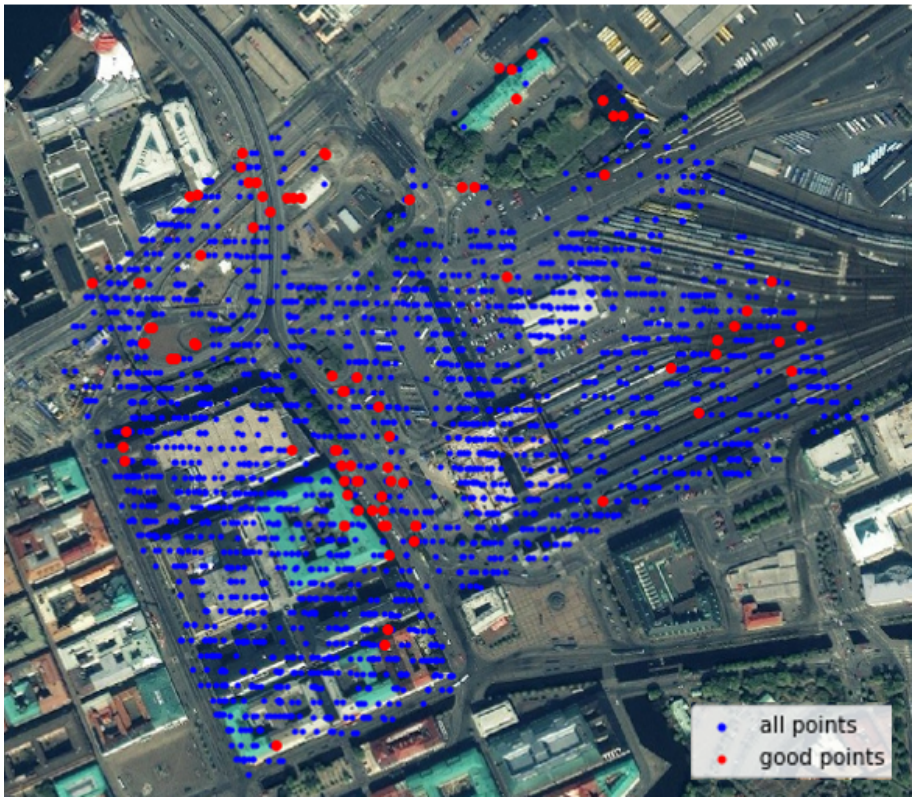

Figure 5.1: InSAR data points, Nordstan/Centralen. Good: points with R^2>0.75

In order to visualize how the quality of points is geographically distributed, hence to see whether their spreading follows a particular pattern, the points characterized by a R^2>0.75 have been plotted on a base-map of the correspondent study site. Figures 5.1 and 5.2 illustrate the results for Nordstan/Centralen and Frihamnen respectively.

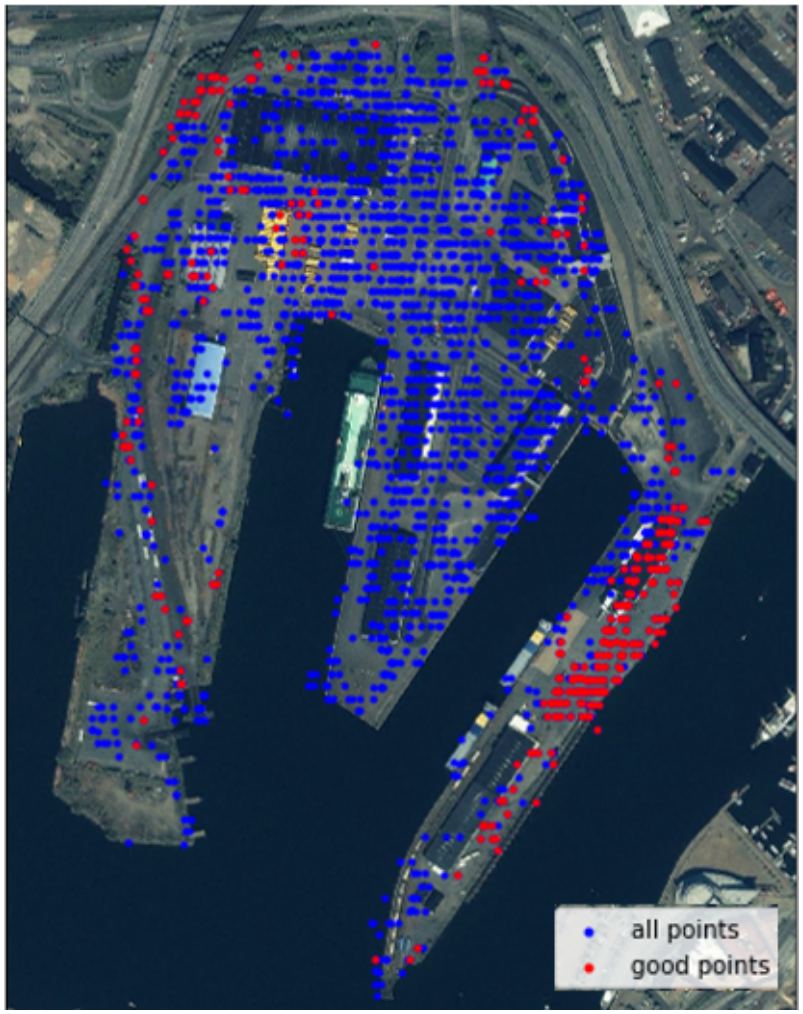

Figure 5.2: InSAR data points, Frihamnen. Good: points with R^2>0.75

As already seen in the previous tables, the two above figures confirm the fact that within an InSAR data-set, high quality data points are not equally spread, being more grouped in high- and low-quality trend areas.
Table 5.11 shows how the density of data points changes depending on the quality level of the points taken into consideration.

Table 5.11: Relation between density and quality of InSAR data points

	Area relying on 1 data point [m^2]			
Study site	Entire data-set	R^2>0.50	R^2>0.75	R^2>0.90
Nordstan	125	909	3541	38073
Frihamnen	207	752	1450	4662

It is possible to see from the above table how the average density of data points drops drastically when filtering out low quality ones. Nordstan shows a decrease of almost 10 times for each points quality class increment, while Frihamnen is characterized by lower, but still consistent, drops in density. The results of the density analysis for Frihamnen study site are visible in Figure 5.3 below in more detail, where a heat-map is generated dividing the area in regular hexagons and showing the number of data points for each hexagon (bin) when considering different quality classes. For space reasons the heat-map for Nordstan can be found in Appendix A (Figure A.3).

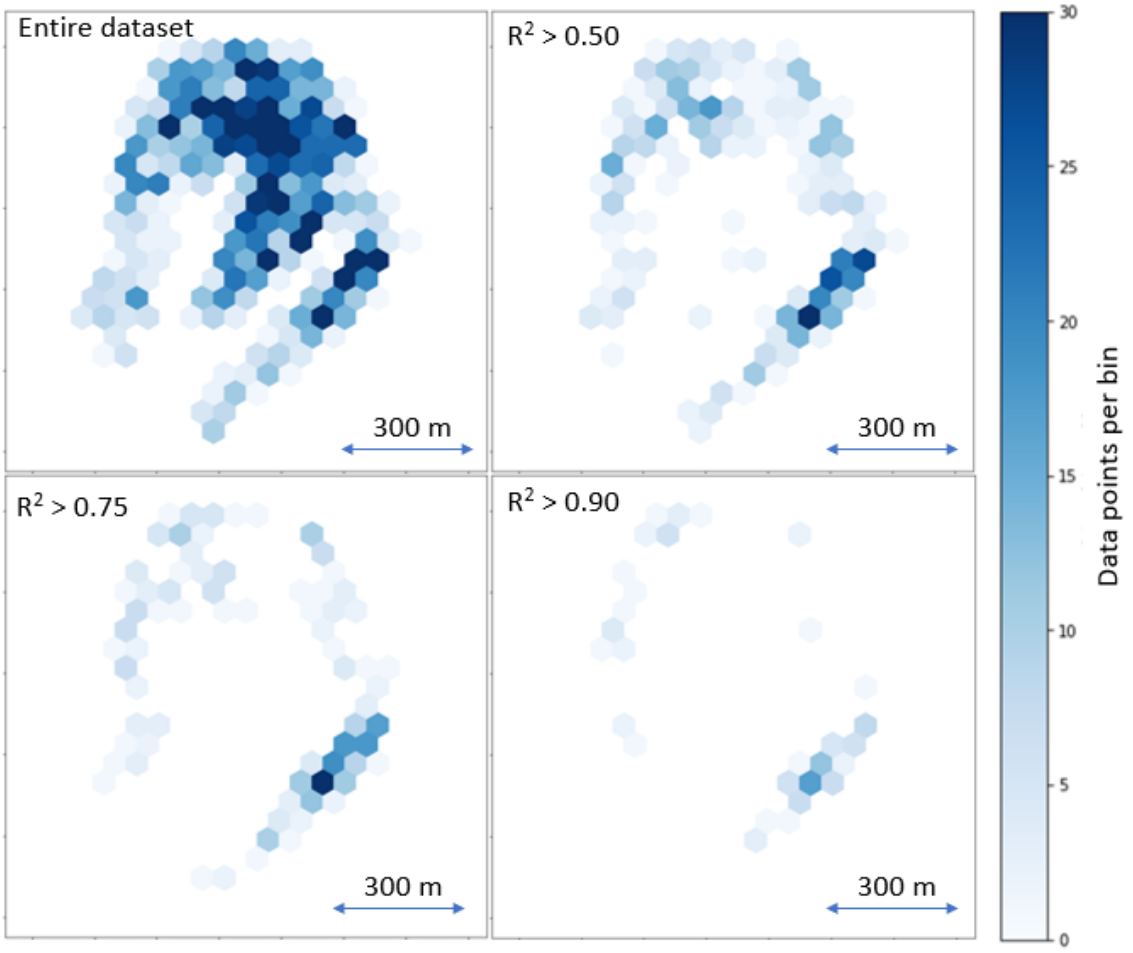

Figure 5.3: Variation of InSAR data points density when considering different quality classes in Frihamnen study site

6

Geotechnical interpretation and discussion

The present chapter concludes the work of this study, trying to find a reason behind the results of the work and presenting many points for reflection and a geotechnical interpretation about the findings. The chapter is followed by the final conclusions, where some ideas for possible further research in this context are presented, that has not been possible to carry out during the present study.

The results presented in Section 5.1, as seen, are characterized by different levels of discrepancy between InSAR measures and traditional methods' ones. In general, many reasons can be found behind these uncertainties, but let us try to go into details for the present results. The simplest case to file is the one presented in Table 5.1; here the reliability of the results depends totally on the quality of a single InSAR data point, ID:821, being the one correspondent to the position of the studied bellow hose gauge. This point, as mentioned already, happens to have a temporal coherence of 0.57, lower than the average data-set's one of 0.7. This parameter, similarly to the R^2 in the linear regression analysis, indicates how consistent in time the measures coming from a specific point are, meaning hence a low quality for point ID:821 and low reliability of its measures. Same reasoning is valid for Table 5.2 coming from the same point. A difference here though is that when taking into consideration the trend-line, the mistaken measurements affect the result less, resulting less evident with the average trend.

There is something that is in general worth mentioning, a possible reason behind the difference in magnitude in the results of Table 5.2 and especially 5.3. When a clayey soil is negatively deforming due to an increment in vertical effective stress, the behaviour of settlement over time is not linear. As shown in the example in Figure 2.3, the displacement results faster during the first period, when the main share of it takes place (steeper trend), while slowly decreasing with time, tending more and more to a linear flat trend, until its final value is reached. This means that if the settlement is measured in two different moments, sufficiently distant in time (this depends on the type of soil), it is normal for the most recent measures to show a decreased settlement trend. This is exactly the case of the present study, where, as mentioned already, InSAR data-set is by years more recent than traditional methods measures, for both the study sites, especially Frihamnen.

A peculiarity of this last study site, Frihamnen, is observed when looking at the

optical levelling measures in Figure A.1 and A.2 (Appendix A). These measures extend on a 60-year-long time period, showing different behaviours for the two piers. Norra Frihamnspiren (Figure A.1) is characterized by a slight settlement during the first measurements period, that then tends to zero during last period. This behaviour could resemble the very last phase of a clayey soil settlement, creep. This assumption results confirmed by the InSAR measurements in the area (Table 5.10), which suggest a settlement value proximate to zero taking place also during their more recent measurement period. Södra Frihamnspiren (Figure A.2) on the other hand, is characterized by a settlement trend that differs from the usual clayey soil behaviour, showing a consistent linear settlement taking place during almost the whole period of optical levelling measurements, that continues also during InSAR more recent measurement period, with a magnitude slightly lower but still consistent (Table 5.10). A geotechnical interpretation of this difference, may find the reason for it in the type of soil that characterizes these two piers' subsurface. As seen in Section 3.2 in fact, Södra Frihamnspiren, because of its position, was built using more organic soil, which normally shows a settlement behaviour consistent in time, different from the clay one. On the contrary, Norra Frihamnspiren lays on a more clayey soil, that hence leads to the observed settlement trend.

Another relevant fact when it comes to the discrepancy found in the comparison results of both Sections 5.1 and 5.2 is represented by the findings of the statistical analysis of InSAR data. These show in fact how the average quality of the InSAR data-sets used for this work is in general low. Only around 28% of points are considered to have an acceptable reliability according to their consistence in time for Frihamnen's data-set. The percentage is even halved when it comes to Nordstan's one, with only around 14% of acceptable data points. This fact can be linked especially to Table 5.3 that depends on group of points, and can lead to less precise results. This is proved also by the fact that when only the better quality points are taken into consideration, the results of the comparison show consistently more similarities, as seen in Section 5.4. Furthermore, the fact is highlighted by the study of the density variation carried out within the statistical analysis, showing a drastic drop of data points density when considering the higher quality classes, as illustrated in Figures 5.3 and A.3.

When carrying out a study like the present one, it is important to remember that not all the possible discrepancies in the results rely on the assessed measures them-self, on their quality or on their reliability. Sometimes it can happen that the surrounding environment could affect the measures, leading to possible mistaken conclusions about the studied method that are on the contrary caused by something else. A concrete example of this is represented by Nordstan study site and the E45 Lilla Bommen - Marieholm project. This infrastructural project involves the realization of a 800-meter-long stretch of highway positioned at a 6-meter depth, in order to facilitate the interconnection with the new infrastructural developments of the area. Around 400 m of this stretch will consist of a tunnel and above this tunnel's roof, some buildings will be built. This means that the foundations for this project need not only to face the weight of the buildings, but also the one coming from the tunnel,

the highway and its traffic. In order to face this, the company working on the project has designed a system of deep foundations consisting of a high number of concrete piles developed by them. They claim that this particular design allows them to use less piles, but still, a total of 275000 m of piles (PEAB, 2019) is being driven into the soil underneath, to different depths. Given that these works are taking place quite close to what is Nordstan/Centralen study site and that they started back in 2015, with the main production going on since 2016, it is assumed to be possible that the InSAR soil displacement measures in Nordstan study site have been affected by this. In fact in general, when piles are pushed into the soil, the surrounding areas could be affected by soil displacement, precisely heave, with varying magnitudes. If this is the case for Nordstan study site, this might represent a further reason behind the difference in magnitude of the measures comparison. A proof of this is given by Figure 4.4, where is possible to see how most data points measuring heave are found in the north-east area of the site (especially the trend area corresponding to bellow hose B), the closest one to the E45 works.

For what regards the possible use of InSAR measurements combined with Asaoka's "observational procedure", the findings show how the use of this method can lead to a quick and relatively easy estimation of the final settlement value and hence the time needed for it, based on the measures, given the possibility to retrieve the settlement trend from them. It is important to remember though, that the final settlement value retrieved with this method does not include creep, but only immediate settlement and first consolidation. For this reason and the ones discussed above regarding this study site, the prediction that regards Frihamnen is considered less reliable than Nordstan one. In general though, this tool can result of much usefulness in situations where straightforwardness and simplicity are preferable to precision and accuracy for the prediction of the time and magnitude factors of settlement in a specific area. A strength of this method consists of no need for any installation of measuring tools in the area and no need to access the area at all. On the other hand, despite the fact that SAR data are publicly available for free, they do need some knowledge on how to manage them and how to transform their raw data in useful information. Furthermore, another fact that emerges from this analysis is the need for a reliable value for the pore water drainage path when it comes to the retrieving of the coefficient of consolidation through Asaoka's method. The results proved in any case that despite the 8-10% of uncertainty in this value, the resulting c_v agrees with Table 2.1, differing by one order of magnitude from the one suggested by laboratory tests.

In conclusion, some issues on this work's path were related to data availability and data quality. Nevertheless, the study achieved interesting findings and conclusions and the rest of incomplete research questions are left at the end as ideas for possible further research on the subject.

7
Conclusion & Recommendations

The findings of the present study show the interferometric Synthetic Aperture Radar technique to result a valid tool for possible geotechnical applications. On the one hand, this kind of measures need a consistent amount of work in order to transform the raw data into useful and usable information, especially when considering the pre-processing procedure, not treated in the present study, through which the real transformation step is achieved and the vast majority of errors removed. On the other hand, when there is the possibility to invest the time and knowledge needed for processing these data, they have proved to have geotechnical capabilities comparable to the ones of traditional methods for what regards soil displacement monitoring, in addition to settlement prediction potentialities when assisted with hand calculation. InSAR technique is furthermore strengthened by having a huge database of images for measurements averagely covering the last two decades, already available. One of the main findings of this work, results to be the strict relationship between the consistency in time of the InSAR measurements and their accuracy. The statistical analysis has in fact proven how strongly the similarities to traditional methods' results increase when filtering out the lower consistency data points. Furthermore, another related aspect, highlighted by the heat-maps, is the drastic drop in density of data points when considering classes of points with higher quality and better consistency of measurements. This fact is considered the main weakness characterizing InSAR technique, since it leads to a much lower scale of information and hence reliability.

This problem though could be something related only to the data-set used for the present study, covering the Gothenburg area. A comparison with other InSAR data-sets under the point of view of quality-density relation may represent an interesting purpose for further research in this field. Other ideas for further research emerged during the present study but not investigated for reasons of time, are a comparison of results' accuracy when removing seasonality influence (measures taken during winter) after the filtering of lower quality points; a more detailed statistical analysis studying the spatial correlation between data points measurements and a source tracking of their uncertainties; the assessment of possible retrieving of geotechnical aspects like bedrock deepness profiling or sub-surface layering starting from InSAR measurements in a specific area (detailed geotechnical data coverage needed for this).

Bibliography

Asaoka, A. (1978). *Observational procedure of settlement prediction*. Soils and foundations, 18(4), 87-101.

Atkinson, J. (2007). *The Mechanics of Soils and Foundations* (Taylor & Francis, Ed.). McGrow-Hill, Newyork.

Bozozuk, M., & Fellenius, B. H., (1979). *The bellow-hose settlement gauge*. National Research Council of Canada

Bürgmann, R., Rosen, P. A., & Fielding, E. J. (2000). *Synthetic aperture radar interferometry to measure Earth's surface topography and its deformation*. Annual review of earth and planetary sciences, 28(1), 169-209.

Christensson, P. (2006). *GPS Definition*. Retrieved 2019, Jan 29, from: `https://techterms.com`

Das, B. M. (2007). *Principles of Foundation Engineering* (6th ed.). Thomson.

Dinesh, S. V. (2011). *Consolidation of soils*. Technical report, Siddaganga Institute of Technology, Tumkur.

ESA, European Space Agency (2019). *Missions*. Retrieved 2019, May 15, from: `https://sentinel.esa.int/web/sentinel/missions/sentinel-1`

Karstunen, M. (2018). *Infrastructural geo engineering (BMT041)*. Retrieved from lectures slides, academic year 2018/2019.

Kempfert, H. G., & Gebreselassie, B. (2006). *Excavations and foundations in soft soils*. Springer Science & Business Media.

Knappett, J., & Craig, R. F. (2012). *Craig's soil mechanics* (8th ed.). Abingdon, Oxon: Spon Press.

McCormack, H., Thomas, A., & Solomon, I. (2011). *The capabilities and limitations of satellite InSAR and terrestrial radar interferometry*. Fugro NPA Limited, United Kingdom. Fugro Geotechnical Services Limited, Hong Kong.

Moritz, L. (1995). *Geotechnical properties of clay at elevated temperatures* (Vol. 47). Linköping, Sweden: Swedish Geotechnical Institute.

PEAB (2019). *E45 Lilla Bommen – Marieholm*. Retrieved 2019, Jun 4, from: `https://peab.se/projekt/infrastruktur/e45-lilla-bommen-marieholm/`

SGU, Sveriges Geologiska Undersökning (2019). *Kartvisare*. Retrieved 2019,

Jan 23, from: https://apps.sgu.se/kartvisare/

SMHI, Svenska Meteorologiska och Hydrologiska Institutet (2019). *Ladda ner meteorologiska observationer*. Retrieved 2019, Apr 4, from: https://www.smhi.se/klimatdata/meteorologi/

Terzaghi, K., & Fröhlich, O. (1936). *Theorie der Setzung von Tonschichten*. Vienna.

Verruijt, A., & Van Baars, S. (2007). *Soil mechanics* (pp. 19-25). Delft, the Netherlands: VSSD.

Wager, O. (1973). *Measuring vertical movements in soil by means of a bellow hose*. Norwegian Geotechnical Institute.

A
Appendix 1

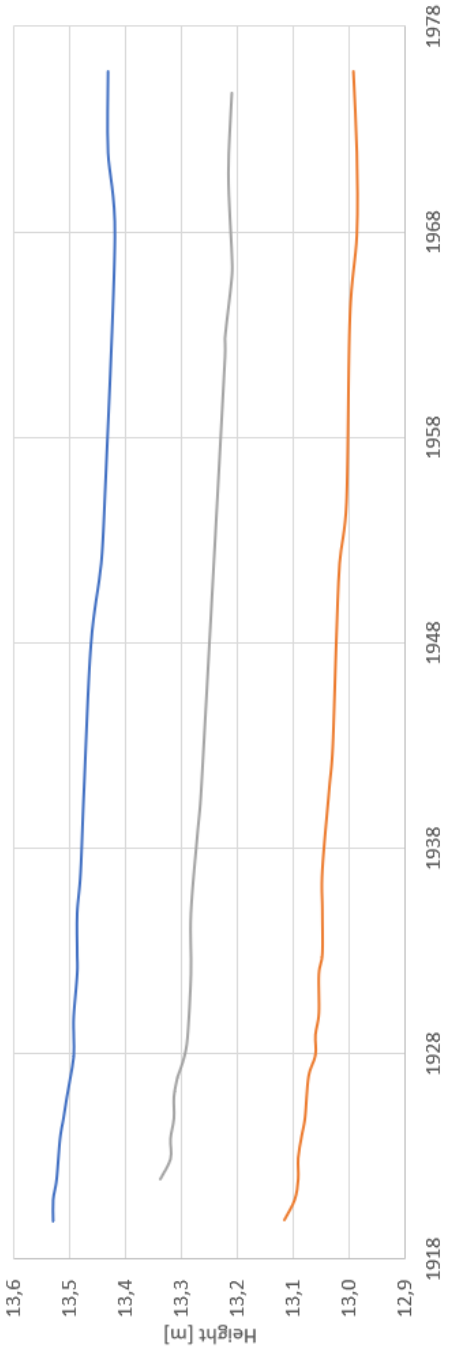

Figure A.1: Optical levelling measurements in Norra Frihamnspiren

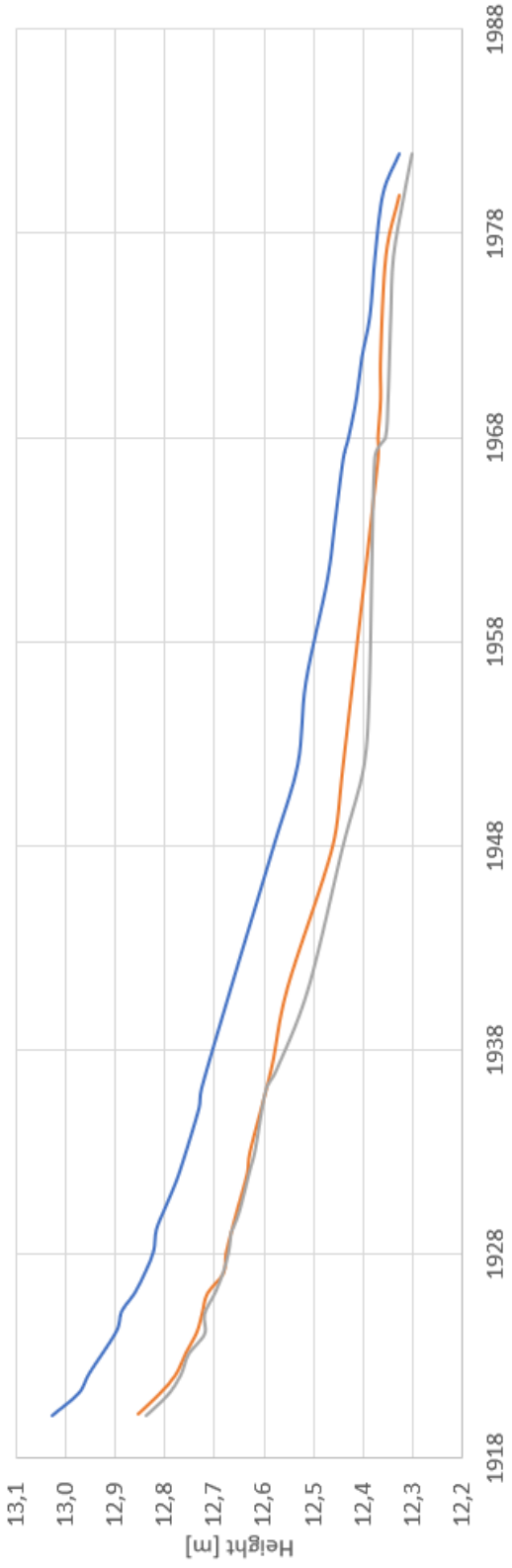

Figure A.2: Optical levelling measurements in Södra Frihamnspiren

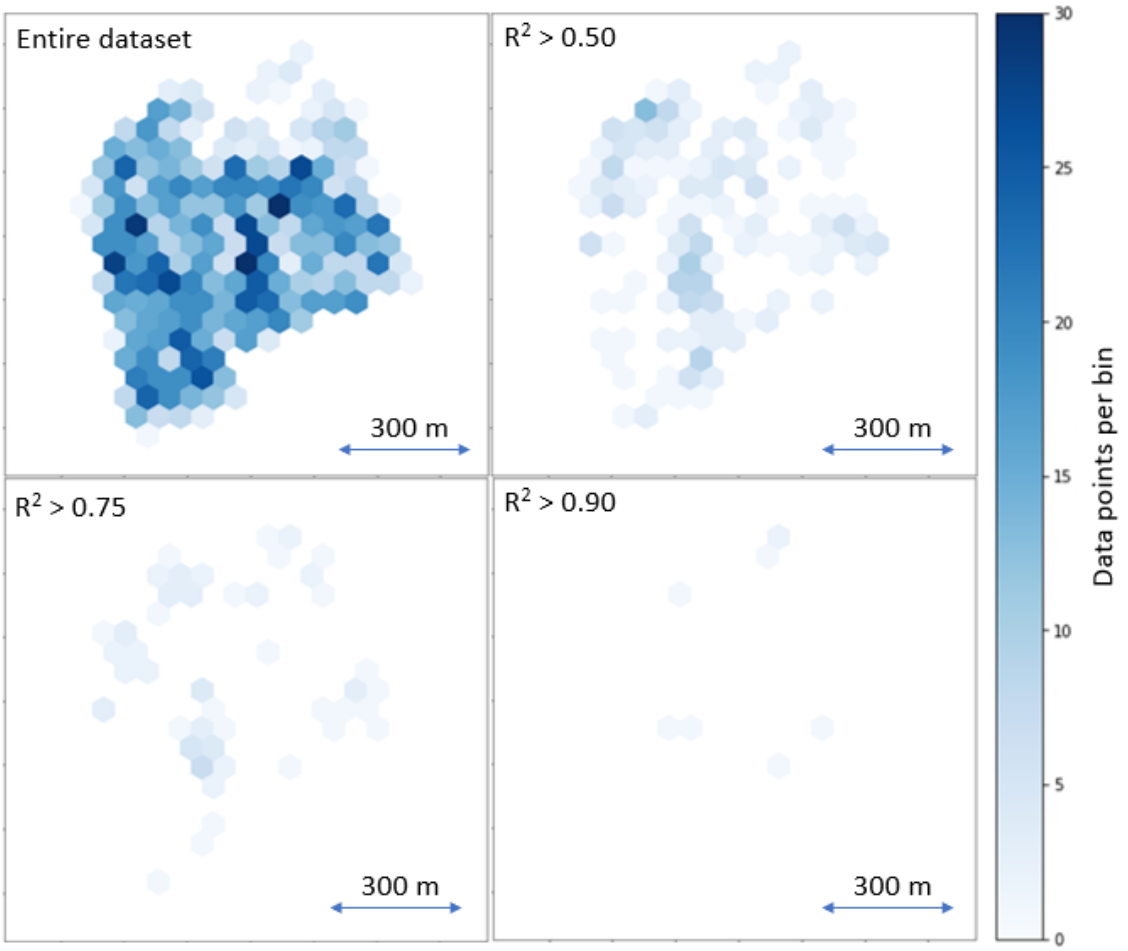

Figure A.3: Variation of InSAR data points density when considering different quality classes in Nordstan study site

B

Appendix 2

Python code used for section 4.4:

```
import numpy as np
from sklearn.linear_model import LinearRegression
import pandas as pd
import matplotlib.pyplot as plt
from mpl_toolkits.basemap import Basemap

#import InSAR csv file
df = pd.read_csv(
"C:/Users/maquin/Documents/Site choice/Frihamnen/SAR_Frihamnen_new.csv")
print('Frihamnen')
#df = pd.read_csv(
#"C:/Users/maquin/Documents/Site choice/Nordstan/SAR_Nordstan_new.csv")
#print('Nordstan/Centralen')

#create deformation measurements dataframe (y)
insar_points2 = df.iloc[0:-1,18:]

#create dates array (x)
dates = np.array(df.iloc[-1,18:]).reshape(-1, 1)
dates = dates.astype('float64')

#carry out linear regression for each data point
#and calculate rsq and slope for each trend line
def linregrrsq(x):
   return [LinearRegression().fit(dates, x).score(dates, x)]

rsq = insar_points2.apply(linregrrsq, axis=1)

rsq1=[]
for sublist in rsq:
    for val in sublist:
        rsq1.append(val)

def linregrcoef(x):
   return [LinearRegression().fit(dates, x).coef_]
```

```
coef = insar_points2.apply(linregrcoef, axis=1)

coef1=[]
for sublist in coef:
   for val in sublist:
        coef1.append(val)

coef2=[]
for sublist in coef1:
   for val in sublist:
        coef2.append(val)

#add rsq and slope columns to dataframe plus lat and lon
dfs = df.iloc[0:-1,:]
insar_points2['rsq']=rsq1
insar_points2['slope']=coef2
insar_points2['latitude']=dfs.latitude.values
insar_points2['longitude']=dfs.longitude.values

#select points of interest depending on rsq (3 classes)
rsq_50 = insar_points2.iloc[insar_points2.rsq.values >= 0.5]
rsq_75 = insar_points2.iloc[insar_points2.rsq.values >= 0.75]
rsq_90 = insar_points2.iloc[insar_points2.rsq.values >= 0.9]

#calculate median settlement trend for each class of points
trend50 = rsq_50['slope'].median()*365
trend75 = rsq_75['slope'].median()*365
trend90 = rsq_90['slope'].median()*365

#print results
print('The n of points with r_sq > 0.50 is:', rsq_50.rsq.shape[0],
      "%.2f" % (rsq_50.rsq.shape[0]*100/df.shape[0]), '%',
      'and their median trend is:', "%.2f" % trend50, '[mm/year]')
print('The n of points with r_sq > 0.75 is:', rsq_75.rsq.shape[0],
      "%.2f" % (rsq_75.rsq.shape[0]*100/df.shape[0]), '%',
      'and their median trend is:', "%.2f" % trend75, '[mm/year]')
print('The n of points with r_sq > 0.90 is:', rsq_90.rsq.shape[0],
      "%.2f" % (rsq_90.rsq.shape[0]*100/df.shape[0]), '%',
      'and their median trend is:', "%.2f" % trend90, '[mm/year]')

#select lat and lon for the points scatter plot
lat = insar_points2['latitude'].values
lon = insar_points2['longitude'].values
lat1 = rsq_75['latitude'].values
lon1 = rsq_75['longitude'].values
```

```
# determine range to print based on min, max lat, long of the data
margin_lon = .0025 # buffer to add to the range
margin_lat = .0004 # buffer to add to the range
lat_min, lat_max = min(lat) - margin_lat, max(lat) + margin_lat
lon_min, lon_max = min(lon) - margin_lon, max(lon) + margin_lon

# create base map using ArcGIS
plt.figure(figsize=(16,11))
m = Basemap(llcrnrlon=lon_min,llcrnrlat=lat_min,urcrnrlon=lon_max,
            urcrnrlat=lat_max, epsg=5520)
m.arcgisimage(service='ESRI_Imagery_World_2D',
xpixels = 1500, verbose= True)

# convert lat and long to map projection coordinates
lons, lats = m(lon, lat)
lons1, lats1 = m(lon1, lat1)

#create scatter plot for both data series
m.scatter(lons, lats, c='w', marker=".", label='all points')
m.scatter(lons1, lats1, c='r', marker=".", label='good points')
plt.legend(loc="lower right")

plt.show()
```